HYDROLOGICAL PROCESSES
Hydrol. Process. **19**, 2815–2844 (2005)
Published online 19 April 2005 in Wiley InterScience (www.interscience.wiley.com). DOI: 10.1002/hyp.5788

Raindrop-impact-induced erosion processes and prediction: a review

P. I. A. Kinnell*
School of Resource, Environmental and Heritage Sciences, University of Canberra, Canberra, ACT 2601, Australia

Abstract:

Raindrop-impact-induced erosion is initiated when detachment of soil particles from the surface of the soil results from an expenditure of raindrop energy. Once detachment by raindrop impact has taken place, particles are transported away from the site of the impact by one or more of the following transport processes: drop splash, raindrop-induced flow transport, or transport by flow without stimulation by drop impact. These transport processes exhibit varying efficiencies. Particles that fall back to the surface as a result of gravity produce a layer of pre-detached particles that provides a degree of protection against the detachment of particles from the underlying soil. This, in turn, influences the erodibility of the eroding surface. Good understanding of rainfall erosion processes is necessary if the results of erosion experiments are to be properly interpreted. Current process-based erosion prediction models do not deal with the issue of temporal variations in erodibility during a rainfall event or variabilities in erodibility associated with spatial changes in dominance of the transport processes that follow detachment by drop impact. Although more complex erosion models may deal with issues like this, their complexity and high data requirement may make them unsuitable for use as general prediction tools. Copyright © 2005 John Wiley & Sons, Ltd.

KEY WORDS soil erosion; raindrop impact; erosion processes

INTRODUCTION

Water erosion comprises a number of forms: splash, sheet, rill, and interrill erosion, gully erosion, bank erosion, snowmelt erosion. Of these forms, sheet, rill and interrill erosion are widely observed in agricultural lands, and empirical models like the universal soil loss equation (USLE; Wischmeier and Smith, 1965, 1978) were developed to predict erosion in areas where these forms occur. More recently, more process-based models like that of the Water Erosion Prediction Project (WEPP; Laflen *et al*., 1997) and the European soil erosion model (EUROSEM; Morgan *et al*., 1998) have been developed. These models have been derived from experiments on erosion processes undertaken by many researchers, including those undertaken by me. This paper brings together understandings of raindrop-impact-induced erosion (RIIE) processes drawn from my work and that of other researchers, and describes some mathematical equations that result from these understandings.

RIIE

Rainfall erosion results from the expenditure of the energy of falling raindrops and flowing water when these two agents act either singly or together. Erosion is a process that involves detachment of soil material from the surface of the soil matrix followed by subsequent transport of the detached soil material away from the site of detachment. No erosion occurs unless detachment occurs first. In the context of this paper, RIIE occurs

* Correspondence to: P. I. A. Kinnell, School of Resource, Environmental and Heritage Sciences, University of Canberra, Canberra, ACT 2601, Australia. E-mail: peter.kinnell@canberra.edu.au

Received 17 December 2003
Accepted 19 July 2004

when detachment results from the expenditure of raindrop energy. RIIE is a major factor in interrill and sheet erosion.

As noted above, rainfall erosion results from raindrop impact and flowing water acting either singly or together. In addition to raindrop impact, surface water flows can detach soil material from the surface of the soil matrix. A critical force needs to be exerted by either a raindrop or a flow before detachment occurs. RIIE dominates erosion when the flow does not possess sufficient energy to cause detachment and is not deep enough to protect the soil surface from drop impact.

Transport of detached material may occur as the result of raindrops and flow acting singly or together. As a result, four detachment and transport systems can be identified:

1. Raindrop detachment with transport by raindrop splash (RD-ST).
2. Raindrop detachment with transport by raindrop-induced flow transport (RD-RIFT).
3. Raindrop detachment with transport by flow (RD-FT).
4. Flow detachment with transport by flow (FD-FT).

RD-ST

When erosion is driven by the energy derived from raindrops impacting the soil surface, raindrop energy is used to overcome the bonds that hold particles in the soil surface and may also be used in the transport of the detached particles away from the site of drop impact. One commonly reported transport mechanism is raindrop splash. Raindrop splash moves detached soil particles radially away from the site of detachment. The RD-ST system often operates at the onset of a storm when little or no surface water flow occurs. However, splash transport (ST) is a highly inefficient transport system. If the soil has no slope, material splashed away from the point of impact of one drop is replaced by material splashed by other drops in the surrounding area. If the soil surface has a slope, then material splashed downslope travels further than material splashed upslope, resulting in the net downslope migration of detached material. That downslope migration increases as the slope gradient increases, but it takes many drop impacts to cause much material to move downslope in most cases. Rainfall erosion is either limited by the detachment or transport capacities associated with raindrop impact or surface water flow. RD-ST is a transport limiting process.

RD-RIFT

When water flows develop on the soil surface, raindrops penetrate through the flow to detach soil particles that may then be splashed as a result of the break-up of the drop or alternatively may be lifted into the flow where they move downstream as they fall back to the surface. Subsequent drop impacts lift the particles into the flow again and again, and they move downstream on each occasion. The resulting transport process involves both raindrop impact and flowing water and, because of this, has been called raindrop-induced flow transport (RIFT; Kinnell, 1990). With coarse material, raindrop impact in flowing water may stimulate particles to roll rather than saltate. RIFT is a more efficient transport system than ST. RD-RIFT plays a major role in moving soil material from interrill areas to rills. Splash can also move material from areas not covered by flow to areas where RIFT operates to give RD-ST-RIFT systems. Although RIFT is more efficient than ST, it still requires numerous drop impacts to move material downstream, and RD-RIFT systems are transport limiting.

RD-FT

In many cases, thin surface-water flows have the capacity to move loose material sitting on the surface but may not have the capacity to detach material from within the underlying surface. However, raindrops penetrating the flow may be able to do this. As a result, particles detached by drop impacts are transported downstream without the need for raindrops to be involved in the transport process. This raindrop detachment-flow transport (RD-FT) detachment–transport system is more efficient than RD-RIFT. Often, both RD-RIFT and RD-FT occur simultaneously in the same flows, with coarse material being transported by RIFT and fine material by FT. In effect, RIFT provides flows with a capacity to transport bedload, where without raindrop impact they would lack that capacity.

Figure 1 provides a schematic representation of how the detachment and transport forms vary with raindrop energy e and stream power Ω when raindrop energy and stream power are used as measures of erosive forces associated with impacting raindrops and flowing water respectively. In Figure 1, the critical energy required for raindrops to detach soil particles held in the soil surface by cohesion and interparticle friction is designated e_c. Raindrop detachment (RD) does not occur unless e is equal to or greater than e_c. Interrill erosion and sheet erosion occur in areas where RD dominates detachment. RD-FT occurs when the stream power Ω is equal to or greater than $\Omega_{c(loose)}$, the critical stream power required for the flow to move loose material sitting on the bed.

FD-FT

The critical stream power for flow to detach soil particles held in the soil surface by cohesion and interparticle friction is designated $\Omega_{c(bound)}$. Flow detachment (FD) does not occur unless Ω is equal or greater than $\Omega_{c(bound)}$. Stream power is a hydraulic parameter that varies with flow discharge and slope gradient. Other parameters, such as flow shear stress, could have been used, but the choice of parameter is largely academic.

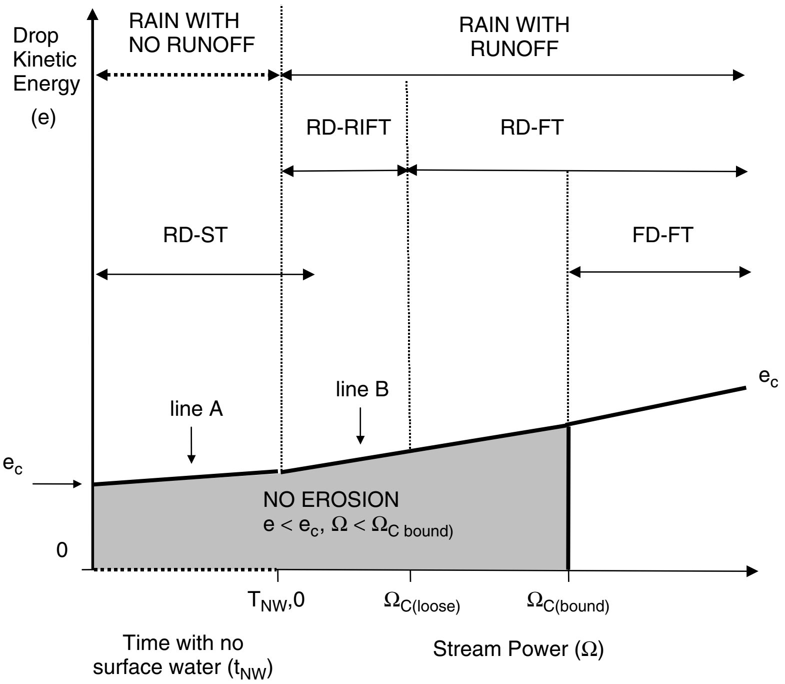

Figure 1. Detachment and transport processes associated with variations in raindrop and flow energies. T_{NW}: total time when rain falls and there is no surface water. e_c: critical raindrop energy to cause detachment; raindrop-induced erosion occurs when drop energy is equal or greater than e_c. A: line for e_c when raindrops are detaching soil particles from the soil surface prior to flow developing. The slope on this line is used to indicate increasing resistance to detachment caused by, for example, crust development. B: line for e_c when raindrops are detaching soil particles from the soil surface when flow has developed. The slope on this line is used to indicate increasing utilization of raindrop energy in penetrating the flow when flow depth increases as flow power increases. $\Omega_{c(loose)}$: critical stream power required to transport loose (pre-detached) soil particles. $\Omega_{c(bound)}$: critical stream power required to detach particles bound within the soil surface (held by cohesion and interparticle friction). RD-ST: raindrop detachment and splash transport. RD-RIFT: raindrop detachment and raindrop-induced flow transport. RD-FT: raindrop detachment and flow transport. FD-FT: flow detachment and flow transport

Consideration of a critical condition for FD remains the same irrespective of which hydraulic parameter is used. Rill erosion occurs where FD occurs.

FACTORS INFLUENCING THE DETACHMENT AND TRANSPORT AMOUNTS

Factors influencing RD-ST

Splash erosion is the common name given to the RD-ST system. For RD to occur when raindrops impact soil surfaces, the kinetic energy e of an impacting raindrop must exceed a critical value (Sharma and Gupta, 1989; Sharma *et al.*, 1991). This is conceptualized through e_c in Figure 1 and

$$D_R = k_D(e - e_c)^b \qquad \text{for } e \geq e_c \tag{1a}$$

$$D_R = 0 \qquad \text{for } e < e_c \tag{1b}$$

where D_R is the weight of soil detached by a raindrop, k_D is the soil detachability coefficient, and b is an empirical parameter. Considering that soils exhibit differing resistances to detachment, e_c can be expected to vary between soil materials. Loose material sitting on the surface is, in this context, essentially predetached, but cohesive forces are involved in holding soil particles within the surface of the soil matrix. In addition to cohesion and interparticle friction, soil moisture also influences the force holding particles within sand (Kinnell, 1974) and soil surfaces (Truman and Bradford, 1990), and hence e_c. Notionally, e_c may also increase during a rainfall event (line A, Figure 1) as a result of surface crusting.

Although the notion of soil particles being detached and transported by the impact of falling raindrops may seem simple, RD-ST involves a series of complex processes. Three stages have been identified for drops impacting soil surfaces not covered by water layers (Terry, 1998):

1. The collision and deformation of a falling raindrop at the soil surface.
2. The rupture and collapse of the drop into a thin disk of fluid spraying radially outwards from the point of impact.
3. The jetting of daughter ejection droplets in parabolic trajectories away from the original drop landing position.

Stages 1 and 2 are involved in the detachment process and in modifying the soil surface characteristics that influence subsequent detachment. How the soil reacts during stages 1 and 2 depends on the physio-chemical properties of the soil (Le Bissonnais, 1990; Romkens *et al.*, 1990). Simple wetting of initially dry soil may produce structural breakdown as a result of internal and external forces associated with water entry into aggregates (Loch, 1995). Hydration of clay particles leads to dispersion in some clay-rich soils, particularly those rich in smectite (Romkens *et al.*, 1990). Drop impacts cause aggregate breakdown (Ghadiri and Payne, 1977) and compaction, resulting in a reduction of soil roughness with time of exposure to rain (Römkens *et al.*, 2001). The effect depends on the kinetic energy of the raindrops and the physio-chemical properties of the soil surface (Moss, 1991a,b; Loch, 1995). Stage 3 provides the transport mechanism for transporting the detached material. Raindrop-impact-induced changes in the soil surface, such as compaction, may influence splash trajectories and, consequently, splash transport.

Splash trajectories are markedly affected by the presence of water layers on the soil surface. Splash angles between 50 and 70° occur with thin water films (Allen, 1987) and tend to become more vertical as the water depth increases. This results in a reduction of the amount of detached material splashed across a boundary as flow depth increases. The presence of water on the surface also affects detachment. Raindrop kinetic energy is absorbed in disturbing water films, leaving less energy available for soil detachment. The effect of flow depth on reducing the amount of energy available for detachment is indicated by e_c increasing as Ω increases in Figure 1 (line B).

Small circular containers known as splash cups have been frequently used to study splash erosion. The surface areas of some cups are usually sufficiently small that all, or nearly all, of the material splashed as a result of a drop impact leaves the confines of the cup. Initially used by Ellison (1944), splash cups have been used by many workers. Ekern (1950) found that drop shape influenced splash erosion in experiments with splash cups filled with sand. Experiments with splash cups may provide data that can be analysed to determine values for factors such as e_c and k_D in Equation (1a). However, as the size of the surface increases, a greater proportion of the material splashed by a drop impact falls back to the surface without crossing the boundary. In a large horizontal area, material splashed away from the point of impact of one drop is replaced by material splashed to that point by impacts in the surrounding area, and so very little of the total material detached by impacting raindrops leaves the area. Under these conditions, the transport efficiency of the system can be considered to be negligible. However, if the surface is sloping, then more material is splashed in the downslope direction than the upslope direction, so that the transport efficiency of the system increases as the slope gradient increases. Even so, there is no guarantee that splash will always move soil material downslope on sloping surfaces under natural conditions. Under natural conditions, wind blowing upslope can more than offset the slope gradient effect.

Conceptually, if wind is not a factor that needs to be considered, the concepts incorporated in Equations (1a) and (1b) can be applied to splash erosion on large surfaces if a transport efficiency term that is dependent on slope gradient is included to give

$$S = k_{sS} E_x f(s_g) \tag{2}$$

where S is the amount of material transported across the downslope boundary in an element of time, k_{sS} is the soil erodibility associated with splash erosion, E_x is the effective rainfall energy applied to the surface by the impacting raindrops during that time, and $f(s_g)$ is a function that varies with slope gradient s_g. It follows from Equations (1a) and (1b) that, given n raindrops impacting the surface during the element of time and that, under both natural and artificial rainfall, many seconds occur between successive impacts at a given point on an eroding surface (Foley and Silburn, 2002), then

$$E_x = \sum_{i=1}^{n} (e_i - e_c)^b \qquad \text{for } e_i \geq e_c \tag{3}$$

where e_i is the kinetic energy of the ith drop. However, because the pre-detached material sitting on the surface provides some protection to the underlaying soil surface and is also splashed by a drop impact, k_{sS} is not equal to a single value of k_D for any given soil. In effect, two extreme values of k_D need to be considered. The first, $k_{D.M}$, applies when there are no pre-detached particles on the surface and drops are detaching only material from within the surface of the soil matrix. The second, $k_{D.PD}$, is the value of k_D that applies when the layer of pre-detached material is too deep for the drop to penetrate it and detach soil material from within the surface of the soil matrix. In this case, only pre-detached material is splashed. If H_{Ra} is the degree of protection provided by the pre-detached material, then

$$k_{sS} = (1 - H_{Ra}) k_{D.M} + H_{Ra} k_{D.PD} \tag{4}$$

if it is assumed that e_c also applies to the pre-detached material. Although that may not be the case, k_{sS}, $k_{D.M}$ and $k_{D.PD}$ are, in effect, empirical parameters, and $k_{D.PD}$ will have a value that tends to compensate for the failure of the assumption.

H_{Ra} will vary in time and space. Given a large flat horizontal surface, H_{Ra} effectively becomes unity over the whole surface under steady conditions because the transport capacity of the RD-ST system is negligible. However, a large, flat tilted surface may also exhibit a k_{sS} value equal to $k_{D.PD}$ under steady conditions despite the fact that H_{Ra} is small at the upslope end of the surface. Although drop impacts at the upslope end of the surface may initially impact a surface that does not have pre-detached particles on it, any subsequent drop impacts downslope of that area will impact a surface that has pre-detached particles sitting on it. Given that any point in space has an equal probability of being impacted, a large number of drop impacts in the surrounding area may contribute to the layer of pre-detached material on the surface before a particular point on the surface is impacted. For example, under natural rainfall, a 1 cm^2 area receives, on average, one drop impact every 5 s when the intensity is 40 mm h^{-1} (Foley and Silburn, 2002); and given that raindrop impact is spatially random, then, on average, around 99 drop impacts may occur in a 10 cm by 10 cm area before the same 1 cm^2 area is impacted a second time. Thus, if $k_{D.PD} > k_{D.M}$, which tends to be the case (since the pre-detached particles are held to the surface by essentially nothing more than gravity), then the upslope drop impacts provide increasing amounts of pre-detached material to downslope drop impacts as one progresses down the plane. The rate of increase in H_{Ra} down the slope depends on the efficiency of the splash transport system: the greater the efficiency, the less the change in H_{Ra} with distance in the downslope direction. However, given a long enough slope, $H_{Ra} = 1$ will occur in the area close to the downslope boundary where the drop impacts that cause splash to pass directly across the downslope boundary occur. It is the value of H_{Ra} in this downslope zone that controls the rate of erosion from the area as a whole. The distance the zone extends upslope from the downslope boundary depends on splash travel distance.

As noted earlier, RD-ST is a transport limiting system. Although $k_{D.PD} > k_{D.M}$ occurs when the particle size and density characteristics of the material in the surface of the soil matrix and the pre-detached particles are the same, the size and density characteristics of the pre-detached material tend to vary in time and space. Coarse material tends to be less easily incorporated into splash, and so tends to become more and more concentrated in the pre-detached material in time. Given sufficient time, the failure to transport coarse material may lead to an erosion pavement. Gravel paths are a prime example of this. Most cultivated agricultural soils do not contain sufficient quantities of coarse material to cause erosion pavements to occur during their productive lifetime. However, erosion pavements occur in some untilled arid and semi-arid lands (Abrahams and Parsons, 1991; Parsons *et al*., 1992; Wainwright *et al*., 1995, 1999).

The effect of slope gradient on the net downslope transport of soil material by splash has been observed to be linear in some cases (Moeyersons and DePloey, 1976) and non-linear in others (Quansah, 1981; Grosh and Jarrett, 1994). When the effect is modelled by

$$Q_{ns} = aE^bG^c \tag{5}$$

where Q_{ns} is the net downslope splashed material, E is the total kinetic energy of the rainfall, G is percentage slope, and a, b, and c are empirically determined constants, Quansah (1981) observed c to vary from 0·7 to 1·0 for sand and loamy sand, and from 1·1 to 1·4 for silt loam, silty clay, clay loam and clay soils. Grosh and Jarrett (1994) observed a value of $c = 2$ with a silty clay loam. Considering Equation (2), Equation (5) uses a in place of k_{sS}, E^b in place of E_x and $f(s) = G^c$. However, considering that H_{Ra} varies with size of the eroding area and with the efficiency of the transport system, the assumption that a does not vary with slope gradient may not be correct, and uncertainty exists about the reliability of applying Equation (5) outside the experimental situation used to determine the values of the empirical constants.

RD-ST may be the only detachment and transport system operating for considerable periods of time in some parts of the landscape during a rainfall event or series of rainfall events. At the onset of a rainstorm, runoff is usually absent, and RD-ST operates alone until runoff becomes effective in contributing to the erosion process. Depending on the soil and climate, considerable amounts of soil material can be detached and splashed during this time. Under these circumstances, RD-ST may be causing modification of the soil surface rather than erosion *per se*. Drop impacts cause aggregate breakdown and compaction, resulting in the development of surface crusts in some soils, particularly silty ones (Moss, 1991a,b). The removal of material from and compaction of microtopographic high points and the transport of detached material to microtopographic low points reduces the roughness of the soil surface. The decline in roughness decreases exponentially with the amount of rainfall energy applied to the soil (Romkens and Wang, 1987). The changes in surface properties generated by RD-ST are important to the subsequent erosion that occurs when surface water develops. The development of surface crusts encourages runoff, but it also produces a soil surface that has a greater resistance to detachment. Reductions in roughness also encourage runoff to occur through the reduction in the volume of the depressions that can store water on the surface. How the surface is modified by RD-ST can have a substantial impact on erosion that occurs when runoff develops.

Factors influencing RD-RIFT

RIFT occurs when flows do not have sufficient energy to move soil material unless raindrops impacting the flow disturb the bed underlying the flow. In the context of Figure 1, this occurs when $\Omega > 0$ but less than $\Omega_{c(loose)}$. In this situation, the impacting raindrops lift particles up from the bed into the flow and these particles then fall in a downstream direction as they return to the bed. Figure 2 provides a simple diagrammatic representation of particle uplift and fall associated with a drop impacting non-turbulent water. The process is analogous to wind blowing splash, the difference being that water rather than air is the fluid involved. Particles lifted into the flow fall back to the bed in response to gravity but move horizontally because the fluid they are falling through is flowing horizontally. In simple terms, the falling particles strive to achieve settling velocities as directed by Stokes' law and horizontal velocities of the same magnitude as the flow. Particle travel distance varies with particle size and density, drop size, flow depth and turbulence. Like the RD-ST system, the material transported across any given boundary by RIFT in a unit of time results from the impact of raindrops that occur in an area that lies within a limited distance of that boundary during that unit of time. That distance is controlled by the distance particles travel after being disturbed by a drop impact. Impacts upstream of that area provide a feed of pre-detached material for transport across the boundary by the drops impacting in that area. Also, like the RD-ST system, the RD-RIFT system is a transport-limited system, and material crossing that boundary comes directly from the surface of the soil and loose material detached by previous drop impacts.

Because the material transported across a boundary by RIFT in a unit of time comes from drops impacting within a limited distance upslope, the sediment discharge for particles of effective size p (the size of a particle of sand that would settle at the same velocity as the actual particle) being transported as a result of the impact of drops of size d is given by

$$q_{sR}(p, d) = M_{pd}(F_d X_{Rpd}) \tag{6}$$

where $q_{sR}(p, d)$ is the mass discharged in unit time, M_{pd} is the mass of the p-sized material lifted into the flow by the drop impact, F_d is the spatially averaged impact frequency for drops of size d, and X_{Rpd} is

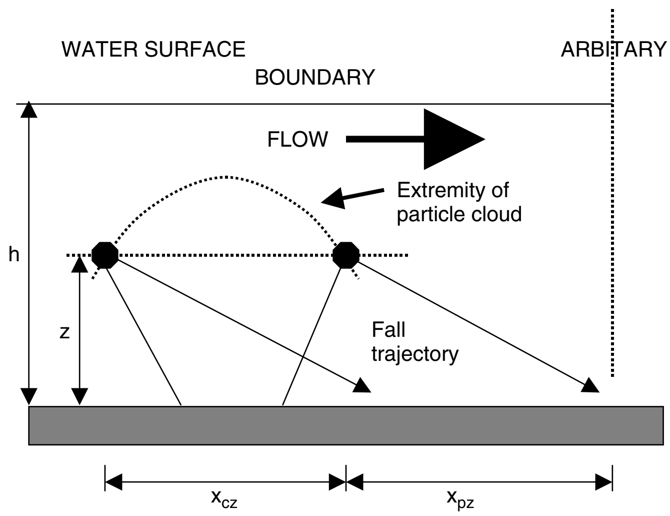

Figure 2. Schematic representation of particle uplift and fall associated with RIFT (after Kinnell (1990)). h: depth of flow; z: height of uplift; X_{cz}: diameter of particle cloud at height z; X_{pz}: horizontal distance particle travels falling from height z

the effective average particle travel distance. Because aggregated material has a lower density than sand, aggregates have a smaller value of p than their actual size. The product of F_d and X_{Rpd} gives the number of drop impacts per unit time that contribute directly to $q_{sR}(p, d)$. Experiments with rain of uniform drop size impacting flows of uniform depth over non-cohesive material (sand) of uniform size showed $q_{sR}(p, d)$ to vary linearly with flow velocity (Kinnell, 1990, 1991). Consequently, X_{Rpd} is linearly influenced by flow velocity. As noted earlier, water depth influences the amount of the energy of the drop impact that reaches the bed. Thus, flow depth influences M_{pd}. Flow depth also affects X_{Rpd}. When flows are extremely shallow, such as at the onset of runoff, flow depth restricts the height to which particles can be lifted in the flow. Consequently, although M_{pd} is high because little of the drop energy is dissipated in the water layer, $q_{sR}(p, d)$ is restricted by X_{Rpd}. As flow depth increase, so does X_{Rpd} and, consequently, $q_{sR}(p, d)$. Variations in the amount of turbulence in the water layer as flow depth varies may influence X_{Rpd}. However, at some stage, impacts no longer have the capacity to lift particles up to the water surface, so that X_{Rpd} then declines as flow depth increases. This decline, together with the reduction in M_{pd} that occurs as more and more of the drop impact energy is absorbed in the flow before particle uplift, causes $q_{sR}(p, d)$ to decline. Eventually, once flows are deep enough, drop impact becomes unable to disturb the bed under the flow. Experiments with drops travelling at or close to their terminal velocity have shown that, for loose sand between 0·1 and 0·9 mm (Kinnell, 1993a)

$$q_{sR}(p, d) = a_p I_d u f(h, d) \tag{7}$$

where a_p is a coefficient that is dependent on particle size and density, I_d is intensity of rain of drops of size d, u is flow velocity, and $f(h, d)$ is a function that varies with flow depth h and drop size d. This function is given by

$$f(h, d) = h \exp(-0.207h) \qquad h < h_c \tag{8a}$$

$$f(h, d) = h \exp[-0.207h - b_d(h - h_c)] \qquad h \geq h_c \tag{8b}$$

when h is in millimetres

$$h_c = 1{\cdot}017 + 4{\cdot}111 \ln(d) \tag{9}$$

and

$$b_d = \exp(0{\cdot}585 - 0{\cdot}387d) \tag{10}$$

when d is in millimetres (Kinnell, 1993a). Figure 3a shows how $f(h, d)$ for 1 to 6 mm drops varies with flow depth. X_{Rpd} is influenced by drop size and particle size and density. For 0·46 mm sand, Kinnell (2001a) observed $X_{Rpd} = 7{\cdot}5$ mm when 2·7 mm drops travelling at near terminal velocity impacted 7 mm deep flows. For coal particles of the same size, $X_{Rpd} = 22{\cdot}2$ mm. From associated experiments with 0·46 mm sand and coal, these values of X_{Rpd} result in M_{pd} of 19 mg and 33 mg respectively. The ratio of the X_{Rpd} values (1 : 2·96) was close to the ratio of the measured settling velocities of the two materials (1 : 2·75). However, in very shallow flows, variations in drop size have negligible influence on the transport of the particles because, as noted above, flow depth restricts X_{Rpd}. That does not mean that $q_{sR}(p, d)$ is not influenced by variations in drop energy when soil surfaces are being eroded under very shallow flows. Although flow depth may restrict the effect of variations in drop size and velocity on X_{Rpd} in very shallow flows, it does not in respect to detachment. Thus, M_{pd} may vary with raindrop energy in very shallow flows over cohesive surfaces when detachment from the surface of the soil matrix occurs within the distance X_{Rpd} of the boundary.

Although sediment discharge is given by Equation (7), it is also given by the product of flow discharge q_w, the mass of water discharged per unit time, and sediment concentration c_s, the mass of material discharged per unit quantity of water. Consequently:

$$q_{sR}(p, d) = q_w c_{sR}(p, d) \tag{11}$$

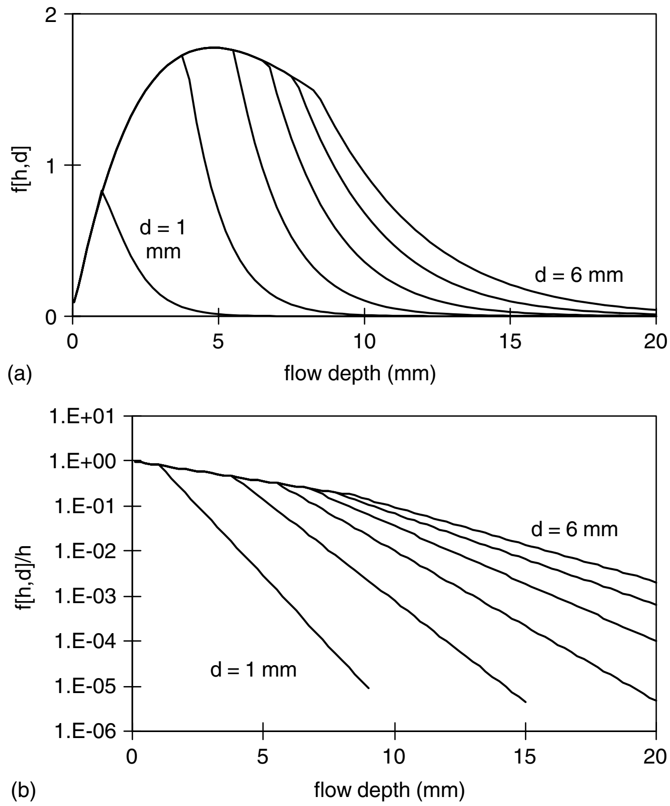

Figure 3. Diagrammatic representations of the effects of flow depth on the flow depth–drop size functions for (a) sediment discharge and (b) sediment concentration resulting from Equations (8) and (14)

where $c_{sR}(p, d)$ is the concentration of p-sized particles associated with the impact of d-sized drops. Under these circumstances, it follows from Equation (7) that

$$q_{sR}(p, d) = q_w a_p I_d f(h, d)/h \tag{12}$$

and

$$c_{sR}(p, d) = a_p I_d f(h, d)/h \tag{13}$$

The flow depth–drop size interaction term associated with sediment transport in Equations (12) and (13) is $f(h, d)/h$. From Equation (8), it follows that

$$f[h, d]/h = \exp(-0.207h) \qquad h < h_c \tag{14a}$$

$$f(h, d)/h = \exp[-0.207h - b_d(h - h_c)] \qquad h \geq h_c \tag{14b}$$

Figure 3b shows how $f(h, d)/h$ varies with drop size and flow depth. It follows from these equations that a_p is the exponent of the 'Y-axis' intercept value obtained when $\ln(c_{sR}(p, d)/I_d)$ is regressed against flow depth when flow depths less than h_c are used. As noted earlier, when flow depths are less than h_c, flow depth restricts X_{Rpd}.

As noted above, like ST, with cohesive soil materials, material transported across the downstream boundary by RIFT may contain both pre-detached material and material from the surface of the soil matrix in the area where the drops impact. Consequently, M_{pd} will vary according to

$$M_{pd} = (1 - H_{\mathrm{Rb}})M_{pd.\mathrm{M}} + H_{\mathrm{Rb}}M_{pd.\mathrm{PD}} \tag{15}$$

where H_{Rb} is the degree of protection provided by the pre-detached material in the area extending a distance $X_{\mathrm{R}pd}$ upstream from the boundary over which the sediment is being discharged, $M_{pd.\mathrm{M}}$ is the mass lifted into the flow when no pre-detached material protects underlying the surface, and $M_{pd.\mathrm{PD}}$ the mass lifted into the flow when pre-detached material fully protects the underlying surface.

Equations (8a)–(10) and (14a) and 14(b) were derived from experiments with beds of loose material where $H_{\mathrm{Rb}} = 1$. For depths greater than h_{c}, Equation (16) has been observed to provide a reasonable model for sediment discharge from both cohesive and non-cohesive surfaces containing a wide range of particle size (Kinnell and Wood, 1992):

$$q_{\mathrm{sR}}(s, d) = 6I_d a_{sd} u(1 - b_d h)/(\pi d^3) \tag{16}$$

where a_{sd} and b_d are empirical factors and u is flow velocity. In Equation (16), a_{sd} is the factor that depends on soil characteristics such as particle size and cohesion of the eroding surface s and drop size d, whereas b_d is a factor that depends only on drop size. For sediment concentration, Equation (16) gives

$$c_{\mathrm{sR}}(s, d) = I_d a_{sd}[6(1 - b_d h)/(\pi d^3 h)] \tag{17}$$

It follows from the comparison between Equations (17) and (13) that the term $[6(1 - b_d h)/(\pi d^3 h)]$ provides a flow depth–drop size interaction term that acts like Equation (14b). However, Kinnell (1993a) observed that Equation (14b) was the better of the two.

The application of Equation (16) to both non-cohesive eroding surfaces and cohesive surfaces containing a wide range of particle sizes indicates that a_p in Equations (12) and 13 can be replaced by k_{sR}, the soil erodibility parameter that applies to the discharge of sediment containing a wide range of particle sizes whether the eroding surface is cohesive or not. Consequently:

$$q_{\mathrm{sR}}(s, d) = k_{\mathrm{sR}} I_d u f(h, d) = k_{\mathrm{sR}} I_d q_{\mathrm{w}} f(h, d)/h \tag{18}$$

where

$$k_{\mathrm{sR}} = (1 - H_{\mathrm{Rb}})k_{\mathrm{R.M}} + H_{\mathrm{Rb}} k_{\mathrm{R.PD}} \tag{19}$$

$k_{\mathrm{R.M}}$ is the value of k_{sR} when there are no pre-detached particles and $k_{\mathrm{R.PD}}$ is the value of k_{sR} when pre-detached particles fully protect the underlying surface.

Equation (19) applies only to RD-RIFT systems, but it is analogous to Equation (4) that applies only to RD-ST systems. Because they apply to a different detachment and transport system, layers of pre-detached materials having the same composition and thickness may produce differing H_{Rb} and H_{Ra} values. Logically, because raindrop energy is absorbed during impact within the water layer, H_{Rb} should vary with flow depth. However, a_{sd} in Equations (16) and (17) was considered constant for any given material in the experiments considered by Kinnell and Wood (1992), so that the effect of any variations of H_{Rb} with flow depth in those experiments was incorporated in the flow depth–drop size interaction terms in Equations (16) and (17). Empirical equations are such that a failure of a term to account for certain conditions can result in another term making up for it. Likewise, if the effect of flow depth on H_{Rb} in Equation (19) is ignored, then it will be incorporated in $f(h, d)$.

Modelling the effect of pre-detached particles

Although variations in H_{Rb} have not been measured experimentally, they have been modelled. Figure 4 shows a schematic of the manner in which Kinnell (1994) simulated particle uplift, downstream travel and return to the bed in a computer model of RD-RIFT on a 100 mm wide by 240 mm long surface. For simplicity,

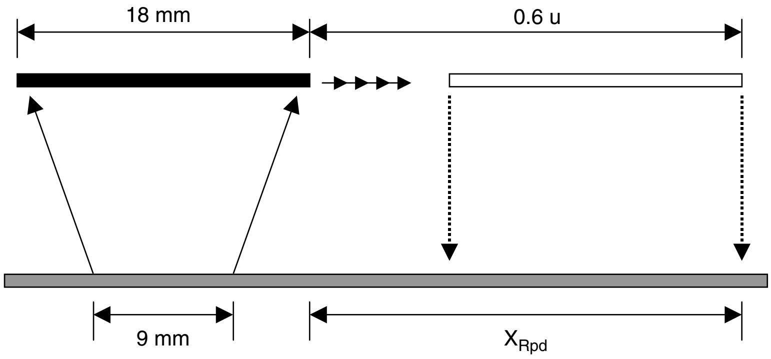

Figure 4. Schematic representation of particle uplift and fall associated with RIFT in the simulation by Kinnell (1994)

the shape of the particle cloud was square and all particles were considered to travel the effective particle travel distance (X_{Rpd}, Equation (6)). This distance was assumed to be 0·6 times the distance the flow moves in 1 s. This was because Kinnell (1990, 1991) observed in previous experiments that particles of 0·25 mm sand impacted by 5·1 mm drops impacting flows produced clouds about 20 mm in diameter and the particles remained suspended for about 0·6 s. The drop impact points were randomly selected during the computer simulation. The amount of material detached from the surface of the soil matrix and lifted (M_S) into the cloud when no pre-detached particles were on the surface was set at a fraction of the maximum amount that the cloud could contain (M_M). Preference was given to uplifting pre-detached particles, and H_{Rb} varied depending on ratio of the amount of pre-detached material available to be lifted into the cloud to the capacity of the cloud. Figure 5a shows how H_{Rb} varied along the eroding surface with flow velocity after 72 000 impacts when $M_S/M_M = 0{\cdot}2$. Figure 5b shows how H_{Rb} varied along the eroding surface with M_S/M_M after 72 000 impacts when the flow velocity was 20 mm s^{-1}. As to be expected, the simulation showed that H_{Rb} increased in the downstream direction. For low velocity flow and high M_S/M_M, the initial increase with distance was considerable, but this was reduced as H_{RB} tended towards 1·0. The increase in H_{Rb} with distance was reduced by increasing flow velocity and decreasing M_S/M_M. Consequently, high cohesion in the soil matrix will tend to produce low values of H_{Rb}.

Simulation of individual drop impact events can only be done on a small scale. Numerical models of surface-water flows often use finite difference techniques that can provide a framework for modelling RD-RIFT. Given certain assumptions, mass balance techniques can be used to determine the sediment transported through and deposited within an element. Figure 6 shows a schematic for the approach used by Kinnell (1994). In this approach, the basic assumptions are:

1. That particles of a particular size are evenly distributed through the depth of flow.
2. That the horizontal vector controlling the trajectory of a particle during its fall is equal to the average flow velocity and the vertical vector is equal to the settling velocity of the particle in water.
3. That particles falling to the surface within the element are evenly deposited over the surface.

Given that the element is of unit width, these assumptions enable the depth of the deposited material z_{Dp} associated with a given particle size p to be calculated from

$$z_{Dp} = q_{sip}/(\rho_D x_{pd}) \tag{20}$$

where q_{sip} is the mass of p-sized particles entering the element in unit time, ρ_D is the bulk density of the deposit and x_{pd} is the average distance p-sized particles travel after being lifted into the flow by the impact of drops of size d. q_{sip} is the sediment discharge (mass per unit width of flow) from the immediate upslope

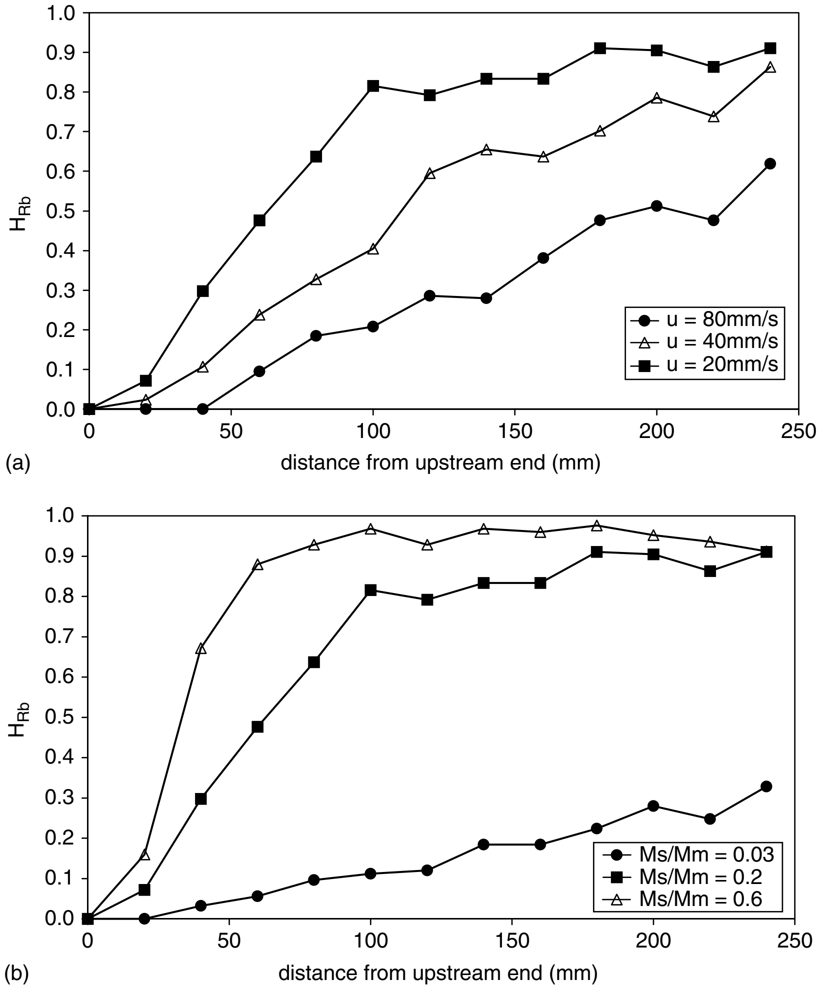

Figure 5. The effect of (a) flow velocity u and (b) the M_s/M_m ratio on H_{Rb} produced by 72 000 simulated drop impacts on a 100 mm by 240 mm cohesive surface using random impacts (after Kinnell (1994)). M_s: mass of particles detached by a drop impact and lifted into the particle cloud when no pre-detached particles exist on the surface; M_m: maximum mass of particles that can be in the particle cloud generated by a drop impact

element. If $q_{\mathrm{so}p\mathrm{H1}}$ is the mass of p-sized material leaving an element when H_{Rb} in the element is equal to 1·0, then the depth of the pre-detached material producing the $H_{\mathrm{Rb}} = 1$ condition ($z_{\mathrm{D}p\mathrm{H1}}$) is given by

$$z_{\mathrm{D}p\mathrm{H1}} = q_{\mathrm{so}p\mathrm{H1}}/(\rho_{\mathrm{D}} x_{pd}) \tag{21}$$

If H_{Rb} varies linearly with the depth of the deposit when $H_{\mathrm{Rb}} < 1$, then it follows from dividing Equation (20) by Equation (21) that

$$H_{\mathrm{Rb}} = q_{\mathrm{si}p}/q_{\mathrm{so}p\mathrm{H1}} \quad q_{\mathrm{si}p} \leq q_{\mathrm{so}p\mathrm{H1}} \tag{22a}$$

$$H_{\mathrm{Rb}} = 1{\cdot}0 \qquad q_{\mathrm{si}p} > q_{\mathrm{so}p\mathrm{H1}} \tag{22b}$$

Equation (18) provides a means for calculating values of $q_{\mathrm{si}p}$ and $q_{\mathrm{so}p}$ (the mass of p-sized particles leaving an element in unit time) when H_{Rb}, $k_{\mathrm{R.M}}$, $k_{\mathrm{R.PD}}$ and the drop size characteristics of the rain are known.

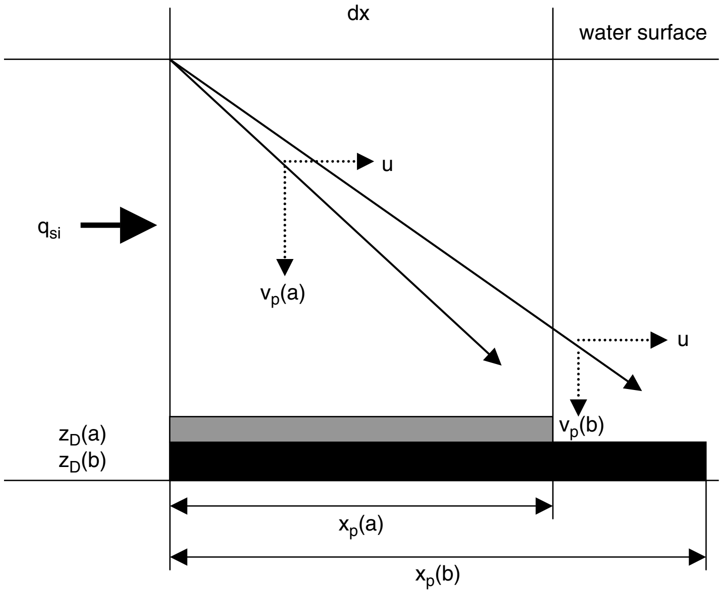

Figure 6. Schematic diagram of travel during deposition of the smallest (b) and largest (a) non-suspended load soil particles entering an element of flow during RIFT (after Kinnell (1994)). q_{si}: the sediment discharge entering the element; $Z_D(a)$: depth of material with particle size *a* deposited on the surface; $Z_D(b)$: depth of material with particle size *b* deposited on the surface. The solid arrowed lines that originate at the top of the water surface show the directions in which particles of size *a* and *b* fall assuming that the horizontal vector is directly related to flow velocity *u* and the vertical vector is directly related to the particle settling velocity v_p; $x_p(a)$ and $x_p(b)$ are the distances particles of size *a* and *b* originating at the water surface travel during their fall; d*x* is the length of the element

Also, the value of q_{sopH1} is given by Equation (18) when $H_{Rb} = 1{\cdot}0$. Thus, given a starting value of H_{Rb}, Equations (18)–(22b) provide the means for modelling H_{Rb} in space and time. Given a situation where the most upstream element has $H_{Rb} = 0$, Kinnell (1994) observed that, under steady conditions, H_{Rb} increased and the composition of the deposited layer became coarser with distance downstream when the approach was applied to a 3 m long surface inclined at 5% under rainfall and $k_{R.M} = 0{\cdot}01 k_{R.PD}$. The sediment discharged by RIFT tends to contain more lighter and finer material than the bed. For example, consider the X_{Rpd} values for 0·46 mm sand and coal noted above. Kinnell (2001a) observed that if each drop impact lifted 60% by mass of sand and 40% by mass of coal, then the proportion of the sediment discharged made up of coal is given by

$$\frac{q_{sR}(p,d)_c}{q_{sR}(p,d)_s + q_{sR}(p,d)_c} = \frac{F_d 0{\cdot}4 M_{pd} 22{\cdot}2}{F_d 0{\cdot}6 M_{pd} 7{\cdot}5 + F_d 0{\cdot}4 M_{pd} 22{\cdot}2} = 0{\cdot}66 \qquad (23)$$

where the subscript 's' indicates sand and the subscript 'c' indicates coal. Thus, given a bed with 40% coal, the sediment discharged by RIFT contains 66% coal.

A mathematical framework for modelling RD-RIFT in a different way was proposed by Rose *et al.* (1983), who proposed that the mass conservation of sediment in size class *i* requires

$$\frac{\partial}{\partial x}(q_w c_i) + \frac{\partial}{\partial t}(h c_i) = r_i - d_i + f_i \qquad (24)$$

where *h* is flow depth, *r* is the rate of rainfall detachment, *d* is the sediment deposition rate, and *f* is the sediment entrainment rate. This framework deals not only with RD-RIFT, but also with RD-FT and FD-FT. For bare soil surfaces, Rose *et al.* (1983) proposed that

$$r_i = a C_r I^p / N \qquad (25)$$

where a is a soil-related coefficient, C_r is the fraction of the soil that is unprotected, p is an exponent originally thought to be close to 2 but now considered to be approximately 1 (Proffitt *et al.*, 1991), N is the number of sediment size classes being considered. N appears in Equation (24) as a result of the stipulation that $c_i = c/N$. In terms of Equation (24),

$$d_i = \alpha_i v_{pi} c_i \tag{26}$$

where v_{pi} is the mean settling velocity in water of particles in size class i, $\alpha_i c_i$ is the sediment concentration close to the bed, and c_i is the depth-averaged sediment concentration (Hairsine and Rose, 1991). According to Rose *et al.* (1983), the steady-state solution for c_i in the ordinary differential equations that result from Equations (24)–(26) and $f_i = 0$ (no detachment by flow) is

$$c_i = \frac{aC_r I^p}{N(q'_w + v_{pi})} \tag{27}$$

where q'_w is the water discharged per unit area.

The effect of q'_w in Equation (27) is not in anyway associated with the effect of flow depth on sediment concentration considered earlier in the section on factors influencing RD-RIFT. That is dealt with through the term a (Rose and Hairsine, 1988; Hairsine and Rose, 1991). It simply results from the solution to the differential equations that result from Equations (24)–(26) and, according to Rose *et al.* (1983), the effect of q'_w is frequently extremely small because often $v_i >> q'_w$. Although that may be so, it is contrary to the observations that, when flow depth is held constant, sediment concentrations associated with RIFT are not influenced by flow discharge because there is a direct relationship between q_{sR} and flow velocity (Kinnell, 1988, 1990).

Recognition of the role of pre-detached material in the discharge of sediment when $f_i = 0$ is included by modification of Equation (24):

$$\frac{\partial}{\partial x}(q_w c_i) + \frac{\partial}{\partial t}(hc_i) = r_i + r_{di} - \mathrm{d_i} \tag{28}$$

where r_{di} is the rate at which material is lifted into the flow from the layer of pre-detached particles (Hairsine and Rose, 1991). This equation represents the interactions of the erosion processes shown in Figure 7. According to Hairsine and Rose (1991)

$$r_{di} = H_{Rb} a_{PD} I(M_{PDi}/M_{PD}) \tag{29}$$

where a_{PD} is the value of a when the layer of pre-detached material completely protects the underlying surface against detachment ($H_{Rb} = 1$), M_{PDi} is the mass of material in size class i in the deposited layer and M_{PD} is the total mass of the deposited layer. Hairsine *et al.* (1999) determined H_{Rb} using

$$H_{Rb} = m_{PD}/m_{PD.H1} \tag{30}$$

where m_{PD} is the mass of pre-detached material per unit area of the bed and $m_{PD.H1}$ is the mass of pre-detached material per unit area of the bed when $H_{Rb} = 1$. According to Hairsine *et al.* (1999), for shallow rain-impacted flows where $f_i = 0$ (no entrainment by flow) and $\alpha = 1$ (sediment concentration uniform through the depth of flow), the time-varying solutions to the equation for RD-RIFT, such as those developed by Sander *et al.* (1996), are both complex and computationally demanding. Steady-state solutions, such as those developed by Hairsine and Rose (1991), are less demanding. Although the dynamic nature of the pre-detached layer is a factor, to some large degree, the complexity in applying the Rose *et al.* (1983) approach to unsteady conditions lies in the involvement of sediment concentration in the calculation of the deposition rate, since the sediment concentration is a net effect of particle uplift and deposition. Under the Rose *et al.* (1983) approach, sediment concentration depends on the deposition rate and the deposition rate on sediment concentration. The

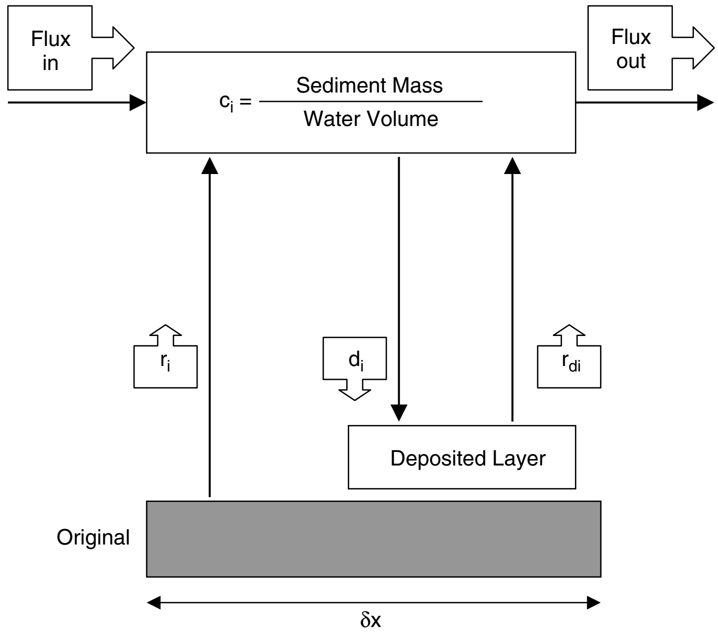

Figure 7. Schematic representation of the effect of deposition rate and the drop detachment rate from the surface of the soil matrix r_i and the deposited layer r_{di} on sediment concentration in the Hairsine and Rose (1991) approach

approach used by Kinnell (1994) does not involve calculating sediment concentration in such a tortuous way and is more easily applied to non-steady conditions.

FACTORS INFLUENCING RD-FT

In RD-FT, particles detached and lifted from the surface of the soil matrix (a) remain suspended in the flow for sufficient time to pass out of the eroding area without returning to the bed, or (b) return to the bed but the flow has sufficient power to move them downstream without aid from raindrop impact. In either case the particle travel distance after being detached by raindrop impact is effectively larger than the distance from where raindrop detachment occurred to the boundary over which the sediment is discharged. Because these particles do not require any aid from raindrop impact, travel downstream is more efficient and faster than particles moving through RIFT. In general, very fine material detached by raindrop impact will be transported by FT, and coarser material moves by RIFT. Thus, both RD-RIFT and RD-FT systems often operate simultaneously in the same flow. When coarse and fine material are detached at the same time, the material moving by FT reaches the end of the eroding area quicker than the material moving by RIFT, and the proportion fine material in the sediment discharged at the onset of a runoff event tends to be high as a result. With time, the proportion of slower moving particles increases, leading to a coarsening of the sediment being discharged. Because the power of the flow to move loose particles varies with flow velocity, the sizes of particles moving via FT and RIFT will vary depending on the flow conditions.

The mass of material detached by a drop impact from the soil matrix that moves by FT ($M_{\text{RD-FT}}$) will, like in the RD-RIFT system, depend on what protection pre-detached particles provide against detachment. Thus, if $M_{\text{RD-FT.M}}$ is the mass detached from the soil matrix by raindrop impact and moved by FT when there are no pre-detached particles:

$$M_{\text{RD-FT}} = (1 - H_{\text{Rb}})M_{\text{RD-FT.M}} \quad (31)$$

While particles moving by FT will not be detached in areas where $H_{\text{Rb}} = 1{\cdot}0$, particles moving by FT will pass over those areas after being detached upstream. Particles travelling by FT may travel at about the same velocity as the flow if they travel as suspended load or at a lower velocity if they saltate. Given a steady state, the discharge of sediment by RD-FT (q_{sRF}) is given by

$$q_{\text{sRF}}(p, d) = (1 - H_{\text{RbX}})M_{\text{RD-FT.M}}(F_d X) \tag{32}$$

where X is the length of flow over the surface where $H_{\text{Rb}} < 1$ and H_{RbX} is effective degree of protection provided by pre-detached particles over the area where $H_{\text{Rb}} < 1$. Equation (32) is similar to the combination of Equations (6) and (15) that applies to RD-RIFT, i.e.

$$q_{\text{sR}}(p, d) = [(1 - H_{\text{Rb}})M_{pd\text{.M}} + H_{\text{Rb}}M_{\text{pd.PD}}](F_d X_{\text{R}pd}) \tag{33}$$

when $H_{\text{Rb}} = 0$, except that X will equal the length of the eroding surface when $H_{\text{Rb}} = 0$ and be reduced as areas where $H_{\text{Rb}} = 1$ develops.

Although X varies with the protective effect of the detached particles travelling by RIFT sitting on the bed, and, as illustrated in Figure 5, that protective effect varies with flow velocity, if that protective effect is absent, then sediment discharges resulting from RD-FT do not vary with flow velocity. In such a case, X equals the length of the eroding area and the term $(1 - H_{\text{RbX}}) = 1{\cdot}0$ so that $q_{\text{sRF}}(p, d)$ is directly related to the product of $M_{\text{RD-FT.M}}$, F_d and the length of the eroding area. The effect can be demonstrated by using a simulation approach similar to that used to produce the RD-RIFT results shown in Figure 5, where particles travel at the velocity of the flow and do not return to the bed before reaching the downstream end of the eroding surface. Figure 8 shows the result of an RD-FT simulation for 50 mm h^{-1} rain with $d = 2$ mm and $M_{\text{RD-FT.M,}} = 4{\cdot}0$ mg for 4 different flow velocities when flow depth was held constant at 5 mm and the horizontally projected area of the cloud was 9 mm × 9 mm. When the flow velocity was 1 mm s^{-1}, $q_{\text{sRF}}(p, d)$ increased linearly once the rain began until it reached the steady-state discharge of 4·0 g m^{-1} s^{-1} after 5 min. When the flow velocity was 100 mm s^{-1}, $q_{\text{sRF}}(p, d)$ increased linearly once the rain began until it reached the steady-state discharge of 4·0 g m^{-1} s^{-1} after 3 s. In both cases, the time to reach the steady-state discharge was given by the time taken for a particle to travel from the upstream end of the eroding surface to the downstream boundary. For 50 mm h^{-1} rain with $d = 2$ mm, $F_d = 3315$ drops/(m^2 s^{-1}) and, thus, 4·0 g

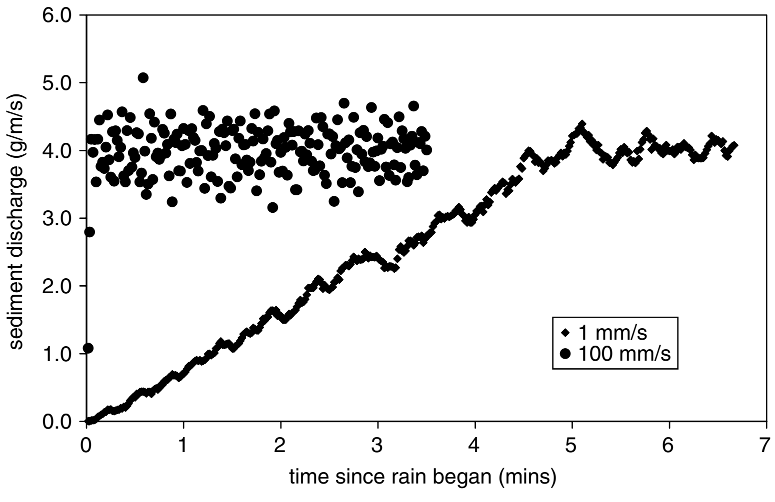

Figure 8. Sediment discharges resulting from a simulation of RD-FT on a 300 mm long by 100 mm wide surface producing only suspended load material when flows 5 mm deep are impacted by 2·0 mm drops with a rainfall intensity of 50 mm h^{-1} and 4·0 mg of material is detached by each drop impact

of material are lifted up from a 300 mm long, 1 m wide surface every second when $M_{RD-FT.M,} = 4{\cdot}0$ mg. Because the steady-state value of $q_{sRF}(p, d)$ remains constant with flow velocity, the sediment concentration varied inversely with flow velocity from 80 g l^{-1} when the flow velocity was 1 m s^{-1} to 0·8 g l^{-1} when the flow velocity was 100 mm s^{-1}. The effect of flow velocity on RD-FT differs from that on RD-RIFT on non-cohesive surfaces (where $q_{sR}(p, d)$ varies directly with flow velocity when flow depth is held constant) simply because of the differing effects of flow velocity of particle travel distance.

Although FT may commonly transport fine material and RIFT systems may commonly transport coarser material detached by raindrop impact on the short slope lengths that are commonly observed in interrill areas, FT may become dominant on relatively short slopes with high slope gradient. Meyer and Harmon (1989) subjected four soils to artificial rainfall using four slope lengths between 150 and 600 mm and four slope gradients between 5 and 30% and observed that micro-rills developed on slopes greater than 10% on some soils as slope length increased but not on others. Obviously, where micro-rills developed, FD-FT, RD-ST, RD-RIFT and RD-FT systems all operated on the eroding areas. However, since loose material requires a lower threshold to become entrained than required to detach material from the soil matrix, Kinnell (2000) suggested that RD-FT became the dominant system operating to discharge sediment on slopes greater 10% as slope length increased when micro-rills did not develop in the Meyer and Harmon (1989) experiments.

Rills tend to develop when the flow detaches material from the surface of the soil matrix but the material actually transported in a rill may contain material originally detached by raindrop impact in interrill areas. It is commonly recognized that detachment by flow (FD) is reduced by the sediment being transported by FT. For example, in the Water Erosion Prediction Project model (WEPP; Flanagan and Nearing, 1995)

$$D_F = K_F(\tau - \tau_0)(1 - q_s/T_{cF}) \tag{34}$$

where D_F is the rate of detachment by flow, K_F is soil erodibility associated with rill erosion, τ is the flow shear stress, τ_0 is a soil-dependent critical shear stress, q_s is the sediment discharge and T_{cF} is the transport capacity of the flow in terms of sediment discharge. In WEPP, it is recognized that detached material entering the rill with interrill flows and splash contribute to q_s and, consequently, if sufficient, may, through the term $(1 - q_s/T_{cF})$ becoming zero, completely suppress detachment by flow. Through this approach, the model deals with the effect of detached material associated with RD-ST, RD-ST-FT, RD-RIFT and RD-RIFT-FT systems on detachment by flow within rills. It should also be noted that though rills may be readily visible in an area, detachment by flow within the rill may be very small or negligible, so that the rills act as nothing more than a transport system for the detached material reaching them via the RD-ST, RD-ST-FT, RD-RIFT and RD-RIFT-FT systems operating in the surrounding areas. Because FT moves such material more efficiently than ST and RIFT, the development of rills on a surface can enhance the rate that material in what has now become an interrill area moves out of that area in comparison with an unrilled area where only sheetflow operates. In effect, rills provide a rapid transport route for material detached by drop impact. Thus, irrespective of any detachment by flow in rills, the development of a rill system can enhance the overall rate of transport of material detached by raindrop impact and, hence, the rate of erosion compared with unrilled areas.

Erodibility variations during rainfall events

Depending on position, an area of soil in an eroding system may be subjected to one or more detachment and transport processes during a rainfall event or a series of rainfall events. Initially, the soil surface may be relatively dry, rough and broken by cultivation. Raindrop impacting the soil surface will modify the characteristics of the surface by causing aggregate break down and compaction as noted in the section on factors affecting RD-ST above. This change in the soil surface characteristics results in the erodibility of the soil changing over time. Until runoff develops, RD-ST is the dominant transport system. Because of the low transport efficiency, RD-ST promotes the development of a loose pre-detached layer of particles even on smooth surfaces. A further change in erodibility takes place as this occurs. The development of the pre-detached layer acts as a pretreatment to the detachment and transport systems that develop later when runoff occurs. That layer becomes the layer of pre-detached particles for RD-RIFT and RD-FT systems that operated when runoff develops. Also, the depth and composition of this layer varies once runoff develops; the consequence may be either an increase in erodibility or a decrease, depending on the characteristics of the eroding surface. Meyer and Harmon (1989) applied a series of rainfalls in experiments on side-slope erosion (150–600 mm long surfaces inclined at 5–30%). The first storm had an intensity of about 71 mm h^{-1} and was applied for 60 min. The second was a 30 min storm at the same intensity applied the following day. Kinnell (2000) observed that, in these experiments, the sediment concentration c_{SS} varied during either the first one or first two storms, indicating that erodibility changed during these events (Figure 9). For some soils, as shown in Figure 9a, the erodibility increased. In others, as shown in Figure 9b, it decreased.

For the Meyer and Harmon (1989) experiments, Kinnell (2000) observed that the relationship between sediment concentration and rainfall intensity I after the first 60 min storm, or after the subsequent 30 min storm, could be expressed by

$$c_{SS} = a + bI \tag{35}$$

where a and b are empirical constants. Consequently, the sediment discharge $q_{S.SS}$ can be expressed by

$$q_{S.SS} = q_w(a/I + b)I \qquad a \neq 0 \tag{36a}$$

$$q_{S.SS} = q_w bI \qquad a = 0 \tag{36b}$$

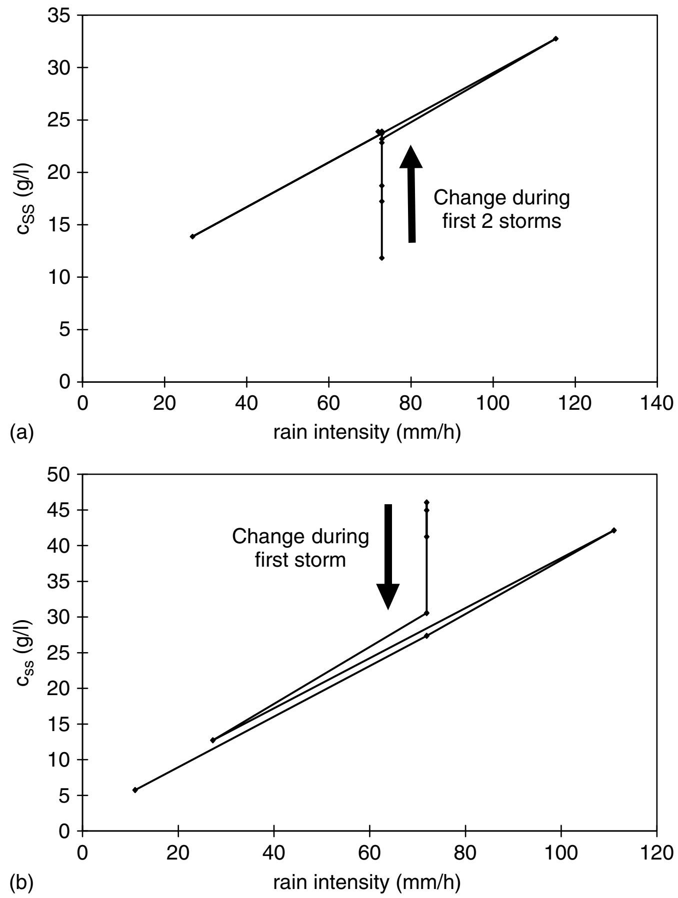

Figure 9. Changes in sediment concentration from side slopes with rainfall intensity during the experiments of Meyer and Harmon (1989) (after Kinnell (2000))

When $a \neq 0$ (e.g. Figure 9a), the term $a/I + b$ in Equation (36a) indicates that erodibility varied after the initial one or two storms. In the majority of the experiments, a did not vary significantly from zero (e.g. Figure 9b), indicating that erodibility reached a steady value after the first one or two storms. However, Kinnell (2000) also observed that, in duplicate experiments on the same soil, the value of b was consistent but that in some cases the value of a could be non-significantly different from zero in one experiment but not in the other. The reason for this difference is essentially unknown and presents some difficulty in developing generalizations except that a significantly greater than zero was more the exception than the rule.

Variations in erodibility during time like those observed by Meyer and Harmon (1989) need to be taken into account when analysing the results of such experiments. Through his analysis of the data when a was not significantly greater than zero, Kinnell (2000) observed results that conflicted with the conclusion of Meyer and Harmon (1989), that soils that do not rill on sideslopes do not produce higher erosion rates as slope length increases. Kinnell (2000) noted that the Meyer and Harmon (1989) analysis was restricted to data obtained during the second storm before the variable-intensity series. He suggested that, had they used the data from the variable-storm series, their conclusion would have been different.

Another example of how experimental procedure needs to be considered when interpreting experimental results is illustrated by Kinnell *et al.* (1996). In a set of experiments where flow depth (3·9–8·2 mm) was used to control the erosive stress on soil produced by rain with uniform drop size (2·7 mm), Kinnell *et al.* (1996) observed that sediment concentration produced by flow depths at the shallow end of the range were higher if the event happened immediately after a common pretreatment (30 min of rain at an intensity between 64 and 77 mm h^{-1} when surfaces were inclined at 5%) than if the surface was subjected to a series of events where flow depth was successively reduced between the events (Figure 10). In the series of events case, all experiments with deeper flows acted as pretreatments to an experiment at a given flow depth, and this caused a build up of coarse material on the surface which led to a reduction in erodibility during the series. The results shown in Figures 9 and 10 indicate that experimental procedure can have a marked effect on results obtained under RD-RIFT plus RD-FT systems and care needs to be exercised in interpreting the results in such circumstances.

The temporal variation in the development of the layer of pre-detached particles and the time taken for particles to move down through RD-RIFT plus RD-FT systems also needs to be considered in some experiments. For example, Zheng *et al.* (2000) reported results from experiments where sediment at a number

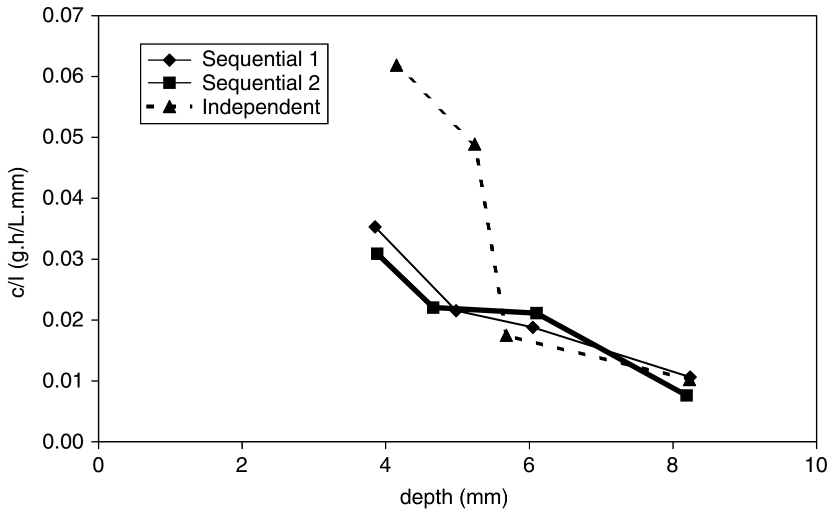

Figure 10. The effect of flow depth on the ratio of sediment concentration to intensity in the Kinnell *et al.* (1996) experiments with surfaces receiving a sequence of rain events (sequential) and surfaces receiving just one rain event after a pretreatment

of different rates (four) was fed into the top end of a 5 m long test box containing soil being subjected to rainfall erosion using artificial rainfall. Their analysis of the data from these experiments centred on mass balances obtained from the runoff and sediment discharges collected from the feeder system (a smaller inclined surface of the same soil material), the test box without feeder input, and the test box with input. Data were collected under drainage and seepage conditions. Under drainage conditions and lower (5%) slope conditions, Zheng *et al*. (2000) concluded that erosion process in the test box changed from a deposition-dominated process to a transport-dominated process as the sediment concentration from the feeder box was decreased. When the slope was increased to 10% or the hydraulic condition changed to seepage condition, they concluded that the erosion process became transport-dominated. The procedure used to generate the data involved subjecting the inclined surfaces of the feeder and test boxes initially to 8 min of rain when the feeder box and the test box were separated, followed by a period of about 7 min when the two surfaces were connected, after which the boxes were disconnected and data collected for a further 2 min. This initial sequence was performed with 100% of the soil surface in the feed box being exposed to the rain. After this, the feed box exposure was cut to 50% and the sequence repeated. The same sequence was then applied after each reduction of test box surface.

The test box was 5 m long and the first samples during the experiments when the input feed was applied were taken 2 to 3 min after the input feed began. Kinnell (2001b) noted that, in the case of a sample being taken at the 3 min mark, only feed particles travelling at or faster than 28 mm s^{-1} would be collected. If the last sample was collected 4 min later, then it would contain feeder particles travelling at 12 mm s^{-1} or more. While the next two samples in the sequence were collected when the feed was removed, they would contain feeder particles travelling first between 12 and 10 mm s^{-1} and then between 10 and 9 mm s^{-1} if the timing sequence was maintained. Four more samples without feeder input were taken before the next time the input feed was applied. The sediment delivered from the test box during the samples associated with the second feed would contain a mixture of fast-moving particles from the new feed and slow-moving particles from the first feed. The situation becomes more and more complicated as the series of experiments on the one surface progresses. As the data used in the analysis may not be for steady-state conditions, Kinnell (2001b) suggested that the mass balance approach used by Zheng *et al*. (2000) may not be valid. Although Zheng and co-workers (Huang *et al*. 2001, 2002) defended their approach, time lags between sediment entering the test box and passing out of it almost certainly influenced their results.

Slope length and gradient effects on the erosion of short planar slopes

As noted earlier, Kinnell (2000) observed results that conflicted with the conclusion of Meyer and Harmon (1989) that soils that do not rill on side slopes do not produce higher erosion rates as slope length increases. Figure 11 shows the effects of slope length on the total erosion produced by the four 15 min storms where intensity was varied on a soil that was not susceptible to rilling and one that was susceptible to rilling. In both cases, erosion increased with slope length when slope gradients were greater than 10% but did not do so when slope gradients were 10% or less. Kinnell (2000) concluded that the effect of increasing slope gradient at slope gradients greater than 10% resulted from an increasing dominance of RD-FT, which was not dominant on the experiments with slopes of 10% and less. The reason for this is that, as slope gradients increase, some particles that were transported by RIFT at lower slope gradients now move by FT because the flow shear stress at a point tends to increase as the distance from the top of the eroding surface and the slope gradient increase. Numerous experiments have been undertaken to determine the effect of slope gradient on interrill erosion, with a wide variety of relationships being demonstrated (Fox and Bryan, 1999). Fox and Bryan (1999) concluded that runoff velocity played an important role in determining the effect of slope gradient on interrill erosion (akin to side-slope erosion) in their experiments. This result is consistent with Equation (7), the equation developed by Kinnell (1993a) for sediment discharges associated with RIFT. Given that the mix of RD-ST, RD-RIFT, RD-FT and FD-FT detachment and transport systems operating on a surface varies not just with slope gradient but also with slope length and the characteristics of the soil, it

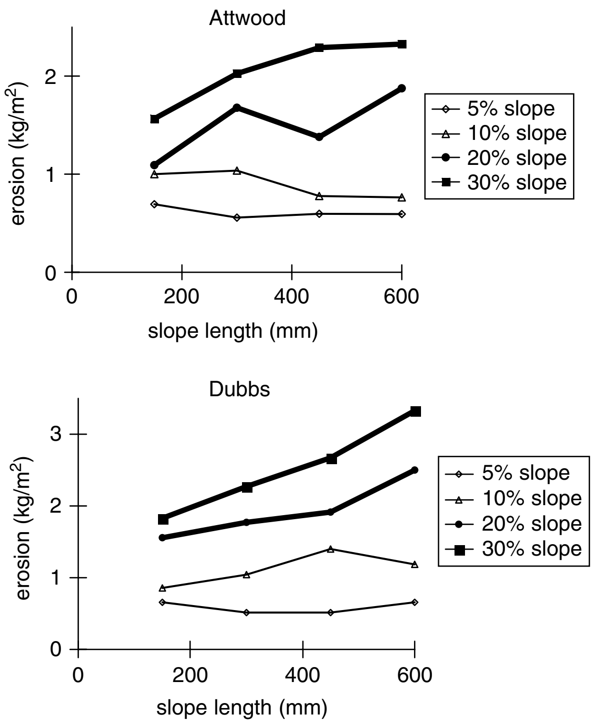

Figure 11. Total erosion for the series of 15 min storms on the Atwood (not susceptible to rilling) and Dubbs (susceptible to rilling) soils determined by Kinnell (2000) from the data reported by Meyer and Harmon (1989)

is unlikely that a single mathematical relationship between slope gradient and interrill erosion can be applied with confidence to all soils.

Factors influencing the measurement of RD

In terms of splash erosion (RD-ST), splash cups have been widely used to examine the capacity of raindrops to cause splash erosion and the resistances of soil materials to being eroded by raindrops impacting surfaces not covered by water. As noted earlier, the splash cup technique was initially used by Ellison (1944) to demonstrate the ability of raindrop impact to cause splash erosion. In many experiments, the materials used have been non-cohesive and well drained and, consequently, the results produced have been indicative of the role of raindrop impact in the transport of pre-detached material. Ekern (1950) showed that drop shape influenced the capacity of raindrops to cause erosion and, as a consequence, experiments using splash cups should involve raindrops falling with their terminal velocity and shape if the results are to relate to splash erosion under natural rainfall. For cohesive soil materials, experiments using splash cups may provide data on raindrop detachment with respect to RD-ST on surfaces not covered by water if the cups are small enough that detached material falling back on to the eroding surface does not have any significant influence on the amounts being splashed. Although this may often appear to be the case, many experiments use rainfall intensities that, in time, lead to ponding and a change in the capacity of raindrops to detach and splash detached material. Irrespective of the effect of ponding on particle travel distances associated with splash, ponding results in some material lifted from the soil surface by a drop impact travelling very short distances within the water layer rather than being splashed. Consequently, ponding encourages the formation of the pre-detached layer, which interferes with detachment. Schultz *et al.* (1985) included detached material sitting on the soil surface in 102 mm diameter containers in their measurements of loss when ponding occurred but took no account of the effect of this material on the detachment rate.

In terms of the measurement of raindrop detachment on non-ponded cohesive soil, Al-Durrah and Bradford (1981) developed an apparatus to collect the splash produced by single drop impact under laboratory conditions. This apparatus, which collected all the splashed material produced by a drop impact, was central to work showing that a linear relationship exists between raindrop detachment and the ratio of drop kinetic energy to soil shear strength (as measured by the fall cone method) (Al-Durrah and Bradford, 1982a) and that soil shear strength influences splash trajectories (Al-Durrah and Bradford, 1982b). Many experiments on raindrop detachment under non-ponded conditions have used splash cups, rather than the Al-Durrah and Bradford apparatus, and in many cases the cup size and the height of the cup rim relative to the eroding surface have influenced the result. Mathematical corrections have been proposed (Farrell *et al.*, 1974; Torri and Poesen, 1988) to deal with these issues, but the problem of not taking account of the effect of loose material on detachment rate is not considered in the approaches.

There are reports (e.g. Torri *et al.*, 1987; Parsons *et al.*, 1994) that have led to the use of splashed soil material as a measure of raindrop detachment under ponded conditions. This implies that the relationship between rainsplash and raindrop detachment is not influenced by factors such as water depth. However, this is not supported by observations on the physics of drop impact. As noted earlier, splash trajectories are markedly affected by the presence of water on the soil surface. The rupture and collapse of the drop into a thin disk of fluid spraying radially outwards from the point of impact followed by the jetting of daughter ejection droplets with low trajectories observed when drops impact non-ponded soil surfaces gives way to crown like structures which produce ejection droplets with much higher trajectories as water depth increases (Macklin and Hobbs, 1969; Moss and Green, 1983). The effect of flow depth on splash trajectory influences particle travel distance and, hence, the proportion of material lifted from the bed that is collected in splash traps. Further increases in water depth to beyond a critical depth result in the cavity carved by the impact of the drop in the water not reaching the underlying bed and a lack of daughter ejection droplets from crown-like structures. However, the subsequent collapse of the cavity produces a vertical jet with a large daughter drop above it and the bed is disturbed when that structure collapses (Moss and Green, 1983). None of the bed material lifted by a drop impact is splashed under these conditions, but some will be discharged with surface water flow. The relationship between splashed material and detached material changes significantly with flow depth, so that splashed material is not a good indicator of detachment under ponded conditions. In addition, the compositions of splashed material and sediment discharged by rain-impacted flow have been observed to differ markedly (Wan and El-Swaify, 1999)

PREDICTING RIIE

At least two more process-based models are currently being promoted as alternatives to empirical models such as the USLE (Wischmeier and Smith, 1965, 1978). One has been developed under the US Department of Agricultural WEPP (Laflen *et al.*, 1997). The other, EUROSEM (Morgan *et al.*, 1998), has been developed in Europe.

The erosion component in WEPP is based on the concept of rills and interrill areas with sediment from interrill areas contributing to the sediment transported in rills. The basic equation used in the WEPP erosion component is a steady-state sediment continuity equation (Flanagan and Nearing, 1995)

$$\frac{dq_s}{dx} = D_I + D_r \tag{37}$$

where D_I is the interrill delivery rate (mass per unit area per unit time) to the rills and D_r is the rill detachment or deposition rate (mass per unit area per unit time). Originally, the interrill delivery rate was modelled using

$$D_I = K_I I_e^2 C_g C_c S_f \tag{38}$$

where K_I is the interrill soil erodibility, I_e is the effective rainfall intensity during the period of rainfall excess, C_g is the ground cover effect adjustment factor, C_c is the canopy cover effect adjustment factor and S_f is a function of the interrill slope:

$$S_f = 1{\cdot}05 - 0{\cdot}85\exp(-4\sin\theta) \quad (39)$$

where θ is the interrill slope angle. K_I values for 18 cropland soils in the western half of the USA were determined experimentally using the I_e^2-based approach with data obtained from experiments with interrill plots under artificial rainfall (Elliott *et al.*, 1989; Liebenow *et al.*, 1990). However, Kinnell (1993b) observed that Equation (39) does not account for the effect of variations in interrill runoff and, consequently, Equation (39) was replaced by

$$D_I = K_I I_e I_x C_g C_c S_f \quad (40)$$

in the 1995 version of the model (Flanagan and Nearing, 1995). In Equation (40), the product of I_e and I_x, the excess rainfall rate, replaces I^2. Since I_x and q_w are directly related to each other, Equation (40) is consistent with Equation (12) if it is assumed that S_f takes account of the effect of flow depth considered in Equation (12). However, the interrill delivery function goes beyond Equation (40) to involve consideration of sediment characteristics through a term known as the interrill sediment delivery ratio (SDR_{RR}). SDD_{RR} is computed as a function of random roughness of the soil surface, the fall velocity of the individual particle size classes, and the particle size distribution of the sediment.

Data from experiments performed by Elliot *et al.* (1989) on 18 US soils were analysed by Kinnell (1993b) to determine soil erodibility k_1 values when

$$D_I = k_1 I q_w S_f \quad (41)$$

There were eight bare interrill plots for each soil in these experiments, six of these were *ridged* plots. These ridged plots had 250 mm side-slope lengths with gradients of about 50 to 60%. In the remaining two, the ridges were smoothed to give *flat* plots. These flat plots had 750 mm slope lengths with gradients of 3 to 8%. The plots were subjected to artificial rainfall at an intensity of about 62 mm h^{-1} over times ranging from 42 to 107 min. Data obtained during the last 5 to 10 min were used in the analysis.

The experiments performed by Elliot *et al.* (1989) were undertaken to provide base-line interrill and rill erodibilities for WEPP. The interrill erodibilities produced by Kinnell (1993b) depend on the inclusion of S_f as determined by Equation (39) within the primary model (Equation (41)). Kinnell observed significant differences between flat and ridged plots with respect to k_1 at $p = 0{\cdot}01$ in six soils, and at $p = 0{\cdot}5$ in six others. Of the 18 soils, only six showed no significant difference in k_1 between flat and ridged plots. These results tend to be consistent with the conclusion that, given that the mix of RD-ST, RD-RIFT, RD-FT and FD-FT detachment and transport systems operating on a surface varies not just with slope gradient but also with slope length and the characteristics of the soil, it is unlikely that a single mathematical relationship between slope gradient and interrill erosion can be applied with confidence to all soils. Also, in many cases the sediment concentrations varied quite markedly during the period used in the analysis, indicating that the soil erodibility had not reached a steady state before that period commenced.

Experiments like those undertaken by Elliot *et al.* (1989) are usually required to determine interrill erodibilities because of the complex nature of RIIE. As noted earlier, the layer of pre-detached particles is a dynamic layer whose effect depends on the transport systems operating on the eroding surface. In addition, cohesion within the surface of the soil matrix is an important factor in influencing detachment. Laboratory analysis of the soil material does not, at this time, provide adequate information to predict interrill erodibilities for use in models like Equation (41) with great certainty. However, because the mix of RD-ST, RD-RIFT, RD-FT and FD-FT detachment and transport systems operating on the surface during such experiments is essentially unknown, there may be dangers in applying the results of these experiments outside the conditions under which the experiments were performed.

EUROSEM is designed to simulate sediment transport, erosion and deposition over the land surface by rill and interrill processes in both fields and small catchments (Morgan *et al.*, 1998). In contrast to WEPP, which is a continuous simulation model, EUROSEM is directed towards modelling single events. Morgan *et al.* (1998) suggest that, because of this, the EUROSEM approach simulates the dynamic behaviour of events within a storm and is more compatible with the equations used in process-based modelling of erosion mechanics.

The simulation of erosion in EUROSEM is linked to a water and sediment routing structure such as that provided in KINEROS (Woolhiser *et al.*, 1990). The KINEROS model represents the land surface in a catchment as a series of interlinked uniform sloping planes and channel elements. Soil loss is computed through determination of the sediment discharged passing a given point in a given time. The computation is based on the mass balance equation

$$\frac{\partial(AC)}{\partial t} + \frac{\partial(QC)}{\partial x} - \mathrm{DR} - \mathrm{DF} = q_s(x, t) \tag{42}$$

where C is the sediment concentration, A is the cross-sectional area of the flow, Q is the flow discharge, DR is the rate of particle detachment by raindrop impact, DF is the net rate of particle detachment by flow (positive for detachment, negative for deposition), q_s is the external input or extraction of sediment per unit length of flow, x is the horizontal distance and t is time. Traditional concepts of rill and interrill processes are not adopted in EUROSEM. Instead, raindrop and flow processes are modelled on all areas with the distinction between rill and interrill areas being one of geometry. Rills are described as trapezoidal channels, and interrill areas are surfaces without orientated roughness. If rills are present, then EUROSEM assumes interrill areas to slope towards the rills rather than straight downslope. Detachment by rainfall is modelled using

$$\mathrm{DR} = \frac{k}{\rho_s}\mathrm{KE}\ \mathrm{e}^{-zh} \tag{43}$$

where k is an index of the detachability of the soil for which values must be obtained experimentally, ρ_s is the particle density, KE is the kinetic energy of the raindrops impacting the ground surface, z is an exponent varying with soil texture and h is the mean depth of the water layer. Detachment by flow is modelled by

$$\mathrm{DF} = \beta w v_s(\mathrm{TC} - C) \tag{44}$$

where β is the flow detachment efficiency factor, w is the flow width, v_s is the particle settling velocity, and TC is the transport capacity of the flow. TC values for rill flow are calculated from relationships developed for the work of Govers (1990) and for interrill flow from the work of Everaert (1991). With detachment by raindrop impact and flow considered to operate together in the same space, changes in dominance of DR and DF occur with the stream power of the flow (because this determines TC in rill flow) and flow depth (because DR decreases with flow depth).

The equations used in EUROSEM can, in some cases, be seen to represent the processes involved inadequately. For example, the transport capacity of interrill flow is determined without consideration of the influence of rainfall characteristics when rainfall characteristics are known to influence interrill flow transport capacity (Kinnell, 1990). Also, the coefficients used in Equation (43) result from measurement of soil material transported by splash under ponded conditions in the experiments of Torri *et al.* (1987). As noted in the section on the measurement of RD, the water-depth-dependent relationships for splash and RD are not the same, and the approach used in EUROSEM underestimates the amount of material detached by raindrops impacting the soil under the water layer. The resulting bias towards DF means that EUROSEM almost certainly underrepresents the influence of raindrop impact in the areas where raindrop impact is, in reality, an important contributor to erosion.

All current so-called process-based erosion prediction models can be seen to represent the processes involved inadequately in some respect. It is difficult to ascertain how much an effect this may have in many cases because, in the case of RIIE, the mix of detachment and transport systems in the experiments leading to their development or paramaterization is unknown. Also, they do not usually allow for temporal variations in erodibility during a rainfall event. The Hairsine and Rose (1991) approach (Equation (28)) does allow for the influence of the layer of pre-detached particles on erodibility, but, as noted earlier, time-varying solutions to the equation for RD-RIFT, such as those developed by Sander *et al*. (1996), are both complex and computationally demanding. Even if less computationally demanding methods are used, a process-based approach may be too demanding for wide use as a prediction tool, particularly if the data requirements are high. In addition, most models apply to planar surfaces and ignore the fact that many natural surfaces may have a microtopography that results in flow passing through a series of shallow pools where particles transported by RIFT may be deposited. However, improved understanding of the processes involved in raindrop-induced erosion may lead to experiments and models that produce more robust erosion prediction tools.

CONCLUSION

RIIE is initiated when detachment of soil particles from the soil surface results from an expenditure of raindrop energy. Once detachment by raindrop impact has taken place, particles are transported away from the site of the impact by one or more transport processes. These transport processes exhibit varying efficiencies. Particles that fall back to the bed as a result of gravity produce a layer of detached particles on the bed during transport by splash and RIFT. That layer provides a degree of protection against detachment of particles from the underlying soil by raindrop impact and flow, and this influences the erodibility of the eroding surface in time and space. The effects of the storage of pre-detached particles on eroding surfaces need to be considered in interpreting the results of experiments involving RIIE.

Current process-based erosion prediction models do not represent all of the erosion processes well. The review presented here focuses on RIIE processes that have been observed to occur under relatively simple controlled experimental environments and concentrates more on the effect of the transport mechanisms and how the raindrop characteristics affect raindrop detachment than how the surface of the soil matrix reacts to raindrop impact. Current process-based models tend to ignore this issue. In addition, none deals with the issue of temporal variations in erodibility during a rainfall event or variabilities in erodibility associated with spatial changes in dominance of the transport processes associated with RIIE. The models also ignore the fact that in many natural situations where RIIE occurs, the eroding surface is not planar but has a microtopography that encourages water to flow though a series of shallow pools where material transported by RIFT may be deposited. While improved understanding of the processes involved in RIIE may lead to experiments and models that produce more robust erosion models, the complexity of these models, and the high data requirements, may not enable them to be easily used as general prediction tools.

APPENDIX: SYMBOLS AND ABBREVIATIONS

Ω	stream power
$\Omega_{c(bound)}$	critical stream power for detaching particles from surface of soil matrix
$\Omega_{c(loose)}$	critical stream power to move pre-detached particles sitting on the bed
α_i	coefficient, which multiplied by c_i gives the sediment concentration of material in the ith particle size class close to the bed.
β	flow detachment efficiency factor
θ	interrill slope angle
τ	flow shear stress
τ_0	critical shear stress for detachment by flow
ρ_D	particle density
ρ_s	particle density

A	cross-sectional area
a	an empirical coefficient or constant
a_p	an empirical coefficient associated with surfaces made up of p-sized particles
a_{sd}	an empirical coefficient associated with a soil being eroded by raindrop impact when RIFT occurs
b	an empirical power or coefficient
b_d	drop-size-dependent empirical coefficient involved in accounting for the effect of flow depth on RIFT
C	sediment concentration
C_c	canopy cover effect adjustment factor for interrill erosion
C_g	ground cover adjustment factor for interrill erosion
C_r	fraction of soil unprotected by pre-detached particles
c	an empirical power or coefficient
c_i	sediment concentration associated with the ith particle size category
c_{ss}	sediment concentration associate with erosion on side slopes
c_{sR}	sediment concentration associated with RIFT
D_F	rate of detachment by flow
D_I	interrill delivery rate
D_r	rill detachment or deposition rate
DF	net rate of particle detachment by flow
DR	rate of particle detachment by raindrop impact
d	drop size
d_i	sediment deposition rate of particles in the ith particle size category
E	total kinetic energy of rainfall
E_x	effective rainfall energy applied to surface by raindrop impact in an element of time
e	kinetic energy of impacting raindrop
e_c	critical raindrop kinetic energy for detaching particles from surface of soil matrix
e_i	kinetic energy of the ith drop
f_i	entrainment rate of particles in the ith particle size category
FD	flow detachment
F_d	spatially averaged impact frequency of drops of size d
FT	flow transport
G	percentage slope
H_{Ra}	degree of protection provided by pre-detached material when raindrop detachment occurs in association with splash transport
H_{Rb}	degree of protection provided by pre-detached material when raindrop detachment occurs in association with RIFT
H_{RbX}	effective degree of protection provided over the area where HRb < 1
h	flow depth
h_c	critical flow depth for a raindrop to lift soil particles into the flow and drop size influence RIFT
I	rainfall intensity
I_d	intensity of rain made up of drops of size d
I_e	effective rainfall intensity during period of excess rainfall
I_x	excess rainfall rate
KE	kinetic energy of raindrops impact the ground surface
K_F	soil erodibility for detachment by flow
K_I	interrill soil erodibility
k	index of detachability of a soil
k_1	interrill soil erodibility when interrill erosivity is expressed in term of the product of rainfall intensity and flow discharge

$k_{D.M}$	soil erodibility associated with RD-ST system when pre-detached particles completely protect the underlying surface
$k_{D.PD}$	soil erodibility associated with RD-ST system when no pre-detached particles are present
k_{sS}	soil erodibility associated with RD-ST system
k_{sR}	soil erodibility associated with RD-RIFT system
M_{pd}	mass of p-sized material lifted into flow by impact of drops of size d
$M_{pd.M}$	mass of p-sized material detached from the surface of the soil matrix and lifted into flow by impact of drops of size d
$M_{pd.PD}$	mass of p sized pre-detached material lifted into flow by impact of drops of size d
M_M or Mm	total mass of material that can be held within the particle cloud produced by a drop impact
$M_{RD\text{-}FT}$	mass of material detached by drop impact and moved by FT
$M_{RD\text{-}FT.M}$	mass of material detached by drop impact and moved by FT when no pre-detached particles are present
M_s or Ms	mass of material lifted into the particle cloud by a drop impact when no pre-detached material is present on the eroding surface
m_{PD}	mass of pre-detached material per unit area of the bed
$m_{PD.H1}$	mass of pre-detached material per unit area of the bed when $H_{Rb} = 1$
N	number of particle size categories
p	usually particle size, but an exponent on the Rose *et al.* approach
Q	flow discharge
Q_{ns}	net downslope splashed material
q_s	sediment discharge
$q_{s.ss}$	sediment discharge from sideslopes
q_{sip}	mass of p-sized material entering an element in unit time
q_{sop}	mass of p-sized material leaving an element in unit time
q_{sopH1}	mass of p-sized material leaving an element in unit time when the pre-detached layer fully protects the underlying surface
q_{sR}	sediment discharge associated with RIFT
q_w	water flow discharge
q'_w	water flow discharge per unit area
RD	raindrop detachment
RIFT	raindrop-induced flow transport
RIIE	raindrop-impact-induced erosion
r_i	rate of detachment of particles in ith particle size category by raindrop impact
r_{di}	rate particles in the ith particle size category in the pre-detached layer are lifted into the flow
S	amount of material transported downslope by drop splash
S_f	factor for the effect of slope gradient on interrill erosion
ST	splash transport
s	an eroding surface having a range of particles sizes and/or densities
s_g	slope gradient
TC	transport capacity of flow
T_{cF}	transport capacity of the flow expressed as sediment discharge
t	time
u	flow velocity
v_p	mean settling velocity in water of particle of size p
v_{pi}	mean settling velocity in water of particles in size class i
v_s	particle settling velocity
w	flow width
X	length of flow over which $H_{Rb} < 1$

X_{Rpd} effective average particle travel distance of p-sized particles lifted into flow by the impact of drops of size d

x distance along the line of flow or slope

x_{pd} average distance p-sized particles travel after being lifted into the flow by the impact of drops of size d

z usually height to which a particle is lifted into the flow by a drop impact, but a power in Equation (43)

z_{Dp} depth of pre-detached particles of size p deposited on the bed

z_{DpH1} depth of pre-detached particles of size p deposited on the bed required to produce full protection of the underlying surface

REFERENCES

Abrahams AD, Parsons AJ. 1991. Resistance to overland flow on a desert pavement and its implications for sediment transport modelling. *Water Resources Research* **27**: 1827–1836.

Al-Durrah M, Bradford JM. 1981. New methods of studying soil detachment due to waterdrop impact. *Soil Science Society of America Journal* **45**: 949–953.

Al-Durrah M, Bradford JM. 1982a. Parameters for describing soil detachment due to single waterdrop impact. *Soil Science Society of America Journal* **46**: 836–840.

Al-Durrah M, Bradford JM. 1982b. Mechanism of raindrop splash on soil surfaces. *Soil Science Society of America Journal* **46**: 1086–1090.

Allen RF. 1987. The mechanism of splashing. *Journal of Colloid and Interface Science* **124**: 836–840.

Ekern PC. 1950. Raindrop impact as a force initiating soil erosion. *Soil Science Society of America Proceedings* **15**: 7–10.

Elliot WJ, Libenow AM, Laflen JM, Kohl KD. 1989. *A compendium of soil erodibility experiments*. Publication No. 3, USDA-ARS National Soil Erosion Laboratory, West Lafayette, IN.

Ellison WD. 1944. Studies of raindrop erosion. *Agricultural Engineering* **25**: 131–136, 181–182.

Everaert W. 1991. Empirical relations for sediment transport capacity of interrill flows. *Earth Surface Processes and Landforms* **16**: 513–532.

Farrell DA, Moldenhauer WC, Larson WE. 1974. Splash correction factors for soil erosion studies. *Soil Society of America Proceedings* **38**: 510–514.

Flanagan DC, Nearing MA (eds). 1995. *USDA–Water Erosion Prediction Project: technical documentation*. NSERL Rep. No. 10. National Soil Erosion Research Laboratory, West Lafayette, IN.

Foley JL, Silburn DM. Hydraulic properties of rain impact surface seals on three clay soils—influence of raindrop impact frequency and rainfall intensity during steady state. *Australian Journal of Soil Research* **40**: 1069–1083.

Fox DM, Bryan RB. 1999. The relationship of soil loss by interrill erosion to slope gradient. *Catena* **38**: 211–222.

Ghadiri H, Payne D. 1977. Raindrop impact stress and the breakdown of soil crumbs. *Journal of Soil Science* **28**: 247–258.

Govers G. 1990. Empirical relationships on the transport capacity of overland flow. *Erosion, Transport and Deposition Processes*, Walking DE, Yair A, Berkowicz S (eds). IAHS Publication No. 189. IAHS Press: Wallingford; 45–63.

Grosh JL, Jarrett AR. 1994. Interrill erosion and runoff on very steep slopes. *Transactions of the American Society of Agricultural Engineers* **37**: 1127–1133.

Hairsine PB, Rose CW. 1991. Rainfall detachment and deposition: sediment transport in the absence of flow-driven processes. *Soil Science Society of America Journal* **55**: 320–324.

Hairsine PB, Sander GC, Rose CW, Parlange J-Y, Hogarth WL, Lisle I, Rouhipour H. 1999. Unsteady soil erosion due to rainfall impact: a model of sediment sorting on a hillslope. *Journal of Hydrology* **220**: 115–128.

Huang C, Norton LD, Zheng F. 2001. Reply to 'Comments on Vertical hydraulic gradient and run-on water and sediment effects on erosion processes and sediment regimes'. *Soil Science Society of America Journal* **65**: 954–956.

Huang C, Norton LD, Zheng F. 2002. Second reply to Kinnell's comments on 'Vertical hydraulic gradient and run-on water and sediment effects on erosion processes and sediment regimes'. *Soil Science Society of America Journal* **66**: 1404–1406.

Kinnell PIA. 1974. Splash erosion: some observations on the splash-cup technique. *Soil Science Society of America Proceedings* **38**: 657–660.

Kinnell PIA. 1988. The influence of flow discharge on sediment concentrations in raindrop induced flow transport. *Australian Journal of Soil Research* **26**: 575–582.

Kinnell PIA. 1990. The mechanics of raindrop induced flow transport. *Australian Journal of Soil Research* **28**: 497–516.

Kinnell PIA. 1991. The effect of flow depth on sediment transport induced by raindrops impacting shallow flows. *Transactions of the American Society of Agricultural Engineers* **34**: 161–168.

Kinnell PIA. 1993a. Sediment concentrations resulting from flow depth/drop size interactions in shallow overland flow. *Transactions of the American Society of Agricultural Engineers* **36**: 1099–1103.

Kinnell PIA. 1993b. Interrill erodibilities based on the rainfall intensity—flow discharge erosivity factor. *Australian Journal of Soil Research* **31**: 319–332.

Kinnell PIA. 1994. The effect of pre-detached particles on soil erodibilities associated with erosion by rain-impacted flows. *Australian Journal of Soil Research* **32**: 127–142.

Kinnell PIA. 2000. The effect of slope length on sediment concentrations associated with side-slope erosion. *Soil Science Society of America Journal* **64**: 1004–1008.

Kinnell PIA. 2001a. Particle travel distances and bed and sediment compositions associated with rain-impacted flows. *Earth Surface Processes and Landforms* **26**: 749–758.
Kinnell PIA. 2001b. Comments on 'Vertical hydraulic gradient and run-on water and sediment effects on erosion processes and sediment regimes'. *Soil Science Society of America Journal* **65**: 952–954.
Kinnell PIA, Wood JT. 1992. Isolating erosivity and erodibility components in erosion by rain-impacted flow. *Transactions of the American Society of Agricultural Engineers* **35**: 201–205.
Kinnell PIA, Ramos MC, Uson A. 1996. Method induced variations in erodibility in erosion experiments with rain-impacted flow. *Australian Journal of Soil Research* **34**: 715–720.
Laflen JJ, Elliott WJ, Flanagan DC, Meyer CR, Nearing MA. 1997. WEPP—predicting water erosion using a process-based model. *Journal of Soil and Water Conservation* **52**: 96–102.
Le Bissonnais Y. 1990. Experimental study and modelling of soil crusting processes. In Bryan RB (ed.). *Soil erosion: Experiment and Models*, Bryan RB (ed.). Catena Supplement 17. Catena-verlag: Cremlin-Destedt, Germany; 13–28.
Liebenow AM, Elliott WJ, Laflen JM, Kohl KD. 1990. Interrill erodibility: collection and analysis of data from cropland soils. *Transactions of the American Society of Agricultural Engineers* **33**: 1882–1888.
Loch RJ. 1995. Structure breakdown on wetting. In *Sealing, Crusting, and Hardsetting Soils: Productivity and Conservation*, So HB, Smith GD, Schafer BM, Loch RJ (eds). The University of Queensland, Brisbane: Australia; 113–131.
Macklin WC, Hobbs PV. 1969. Subsurface phenomena and the splashing of drops in shallow liquids. *Science* **166**: 1107–1108.
Meyer LD, Harmon WC. 1989. How row-sideslope length and steepness affect sideslope erosion. *Transactions of the American Society Agricultural Engineers* **32**: 639–644.
Moeyersons J, DePloey J. 1976. Quantitative data on splash erosion simulated on unvegetated slopes. *Zeitsehrift für Geormorphologie* Neve Folge Supplement Band **25**: 120–131.
Morgan RPC, Quinton JN, Smith RE, Govers G, Poesen JWA, Auerswald K, Chisci G, Torri D, Styczen ME. 1998. The European soil erosion model (EUROSEM): a dynamic approach for predicting sediment transport from fields and small catchments. *Earth Surface Processes and Landforms* **23**: 527–544.
Moss AJ. 1991a. Rain-impact soil crust. 1. Formation on a granite-derived soil. *Australian Journal of Soil Research* **29**: 271–289.
Moss AJ. 1991b. Rain-impact soil crust. 2. Some effects of surface slope, drop size, and soil variation. *Australian Journal of Soil Research* **29**: 291–309.
Moss AJ, Green P. 1983. Movement of solids in air and water by raindrop impact. Effect of drop-size and water-depth variations. *Australian Journal of Soil Research* **21**: 257–269.
Parsons AJ, Abrahams AD, Simanton JR. 1992. Microtopography and soil-surface materials on semi-arid piedmont hillslopes, southern Arizona. *Journal of Arid Environments* **22**: 107–115.
Parsons AJ, Abrahams AD, Wainwright J. 1994. Rainsplash and erosion rates in an interrill area on semi-arid grassland, southern Arizona. *Catena* **22**: 215–226.
Proffitt APB, Rose CW, Hairsine PB. 1991. Rainfall detachment and deposition: experiments with low slopes and significant water depths. *Soil Science Society of America Journal* **55**: 325–332.
Quansah C. 1981. The effect of soil type, slope, rain intensity and their interactions on splash detachment and transport. *Journal of Soil Science* **32**: 215–224.
Romkens MJM, Wang JY. 1987. Soil roughness changes from rainfall. *Transactions of the American Society of Agricultural Engineers* **30**: 101–107.
Römkens MJM, Helming K, Prasad SN. 2001. Soil erosion under different rainfall intensities, surface roughness, and soil water regimes. *Catena* **46**: 103–123.
Romkens MJM, Prasad SN, Whisler FD. 1990. Surface sealing and infiltration. In *Process Studies in Hillslope Hydrology*, Anderson MG, Burt TP (eds). John Wiley: Chapter 5.
Rose CW, Hairsine PB. 1988. Processes of water erosion. In *Flow Transport in the Natural Environment: Advances and Applications*, Steffan WL, Denmead OT (eds). Springer-Verlag: Berlin; 312–326.
Rose CW, Williams JR, Sander GC, Barry DA. 1983. A mathematical model of erosion and deposition processes: I. Theory for a plane land element. *Soil Science Society of America Journal* **47**: 991–995.
Sander GC, Hairsine PB, Rose CW, Cassidy D, Parlange J-Y, Hogarth WL, Lisle IG. 1996. Unsteady soil erosion model, analytical solutions and comparisons with experimental results. *Journal of Hydrology* **178**: 351–367.
Schultz JP, Jarrett AR, Hoover JR. 1985. *Transactions of the American Society of Agricultural Engineers* **28**: 1878–1884.
Sharma PP, Gupta SC. 1989. Sand detachment by single raindrops of varying kinetic energy and momentum. *Soil Science Society of America Journal* **53**: 1005–1010.
Sharma PP, Gupta SC, Rawls WJ. 1991. Soil detachment by single raindrops of varying kinetic energy. *Soil Science Society of America Journal* **55**: 301–307.
Terry JP. 1998. A rainsplash component analysis to define mechanisms of soil detachment and transportation. *Australian Journal of Soil Research* **36**: 525–542.
Torri D, Poesen J. 1988. The effect of cup size on splash detachment and transport measurements. Part II. Theoretical approach. In *Geomorphic Processes in Environments with Strong Seasonal Contrasts. Vol. I: Hillslope Processes*, Imeson AC, Sala M (eds). Catena Supplement 12. Catena Verlag: 127–137.
Torri D, Sfalanga M, Del Sette F. 1987. Splash detachment: runoff depth and soil cohesion. *Catena* **14**: 149–155.
Truman CC, Bradford JM. 1990. Effect of antecedent soil moisture on splash detachment under simulated rainfall. *Soil Science* **150**: 787–798.
Wainwright J, Parsons AJ, Abrahams AD. 1995. Simulation of raindrop erosion and the development of desert pavements. *Earth Surface Processes and Landforms* **20**: 277–291.
Wainwright J, Parsons AJ, Abrahams AD. 1999. Field and computer simulation experiments on the formation of desert pavement. *Earth Surface Processes and Landforms* **24**: 1025–1037.

Wan Y, El-Swaify SA. 1999. Runoff and soil erosion as affected by plastic mulch in a Hawaiian pineapple field. *Soil and Tillage Research* **52**: 29–35.

Wischmeier WC, Smith DD. 1965. *Predicting Rainfall Erosion Losses from Cropland East of the Rocky Mountains*. *Agricultural Handbook* No. 282. US Department of Agriculture: Washington, DC.

Wischmeier WC, Smith DD. 1978. *Predicting Rainfall Erosion Losses—A Guide to Conservation Planning*. *Agricultural Handbook* No. 537. US Department of Agriculture: Washington, DC.

Wischmeier WH, Johnson CB, Cross BV. 1971. A soil erodibility nomograph for farmland and construction sites. *Journal of Soil and Water Conservation* **26**: 189–193.

Woolhiser DA, Smith RE, Goodrich DC. 1990. *KINEROS, a Kinematic Runoff and Erosion Model: Documentation and User Manual*. *USDA-Agricultural Research Service*, ARS-77. US Department of Agriculture: Washington, DC.

Zheng F, Huang C, Norton D. 2000. Vertical hydraulic gradient and run-on water and sediment effects on erosion processes and sediment regimes. *Soil Science Society of America Journal* **64**: 4–11.

